aval Research Laboratory
shington, DC 20375-5000

NRL Memorandum Report 5950

(2)

Spatial Realizations of Ship Radiation and Diffraction Waves in Random Ambient Sea Waves

HENRY T. WANG

Center for Fluid/Structure Interactions
Laboratory for Computational Physics and Fluid Dynamics

May 20, 1987

SECURITY CLASSIFICATION OF THIS PAGE A181286

REPORT DOCUMENTATION PAGE

1a. REPORT SECURITY CLASSIFICATION UNCLASSIFIED	1b RESTRICTIVE MARKINGS
2a. SECURITY CLASSIFICATION AUTHORITY	3. DISTRIBUTION/AVAILABILITY OF REPORT Approved ror public release; distribution unlimited.
2b. DECLASSIFICATION/DOWNGRADING SCHEDULE	
4. PERFORMING ORGANIZATION REPORT NUMBER(S) NRL Memorandum Report 5950	5. MONITORING ORGANIZATION REPORT NUMBER(S)
6a. NAME OF PERFORMING ORGANIZATION Naval Research Laboratory 6b. OFFICE SYMBOL (If applicable) Code 4420	7a. NAME OF MONITORING ORGANIZATION Office of Naval Research
6c. ADDRESS (City, State, and ZIP Code) Washington, DC 20375-5000	7b. ADDRESS (City, State, and ZIP Code) Arlington, VA 22217
8a. NAME OF FUNDING/SPONSORING ORGANIZATION Office of Naval Research 8b. OFFICE SYMBOL (If applicable)	9. PROCUREMENT INSTRUMENT IDENTIFICATION NUMBER
8c. ADDRESS (City, State, and ZIP Code) Arlington, VA 22217	10. SOURCE OF FUNDING NUMBERS PROGRAM ELEMENT NO. 61153N; PROJECT NO.; TASK NO. RR023-01-41; WORK UNIT ACCESSION NO. DN280-006

11. TITLE (Include Security Classification)
Spatial Realizations of Ship Radiation and Diffraction Waves in Random Ambient Sea Waves

12. PERSONAL AUTHOR(S)
Wang, Henry T.

13a. TYPE OF REPORT	13b. TIME COVERED	14. DATE OF REPORT (Year, Month, Day)	15. PAGE COUNT
Interim	FROM _____ TO _____	1987 May 20	40

16. SUPPLEMENTARY NOTATION

17. COSATI CODES			18. SUBJECT TERMS (Continue on reverse if necessary and identify by block number)
FIELD	GROUP	SUB-GROUP	Far field waves, Random ambient sea waves, Radiation and diffraction, Spatial realizations

19. ABSTRACT (Continue on reverse if necessary and identify by block number)

The report presents the calculation procedure and numerical examples for the far field radiation and diffraction waves due to a ship in the presence of a random sea. The procedure essentially consists of extending a previously derived method for the ship waves due to a single exciting wave to the multi-wave random sea.

Wave patterns are calculated for four ship hulls, including the case of a twin hull, in the presence of Sea States 2, 4, and 8. The results are presented in the form of three-dimensional, two-dimensional, and contour plots of the ship, sea, and superposed wave patterns. In a Sea State 4, the three smaller hulls make only a relatively small change to the ambient wave pattern while the CVA59 aircraft carrier makes a large change.

Keywords

20. DISTRIBUTION/AVAILABILITY OF ABSTRACT ☒ UNCLASSIFIED/UNLIMITED ☐ SAME AS RPT ☐ DTIC USERS	21. ABSTRACT SECURITY CLASSIFICATION UNCLASSIFIED
22a. NAME OF RESPONSIBLE INDIVIDUAL Henry T. Wang	22b TELEPHONE (Include Area Code) 202-767-2516 22c. OFFICE SYMBOL Code 4420

DD FORM 1473, 84 MAR 83 APR edition may be used until exhausted
All other editions are obsolete

SECURITY CLASSIFICATION OF THIS PAGE

☆U.S. Government Printing Office: 1985—507-047

CONTENTS

SPATIAL REALIZATIONS OF SHIP RADIATION AND DIFFRACTION WAVES IN RANDOM AMBIENT SEA WAVES

1. INTRODUCTION

The calculation procedure as well as numerical examples for the radiation and diffraction wave patterns caused by a ship at zero forward speed excited by a single sinusoidal ocean wave (of given frequency and heading relative to the ship) have been given by the present author in a previous report [1]. Radiation waves refer to those caused by the six oscillatory modes of motion of the ship, while diffraction waves refer to the scattering of the incident wave by the ship hull, taken to be stationary. It was pointed out in [1] that most of the calculations involving a ship excited by ambient waves have been largely concerned with near field flow quantities such as motions, forces, and wave profiles. However, with the introduction of modern day observation techniques such as airborne and spaceborne Synthetic Aperture Radar (SAR) systems and other methods of remote observation such as infrared (IR) and microwave (MR) radiometry, the interest has been enlarged to include the far field wave pattern. A number of recent studies, such as [2,3], have focused on the far field features of the Kelvin wake, the wave system behind a nonoscillating ship advancing at constant forward speed.

The present work was undertaken to obtain estimates of the far field radiation and diffraction waves of typical ship hulls excited by random seas. Essentially, the previously developed calculation procedure for a single sinusoidal wave is generalized to a random sea, composed of a series of component waves of different frequencies and headings.

The report starts with a summary of the calculation procedure for a single wave component [1]. It is shown that the wavemaking due to all the sources on the hull surface is expressed in terms of the concise and convenient Kochin function. In this summary, as well as throughout the report, the ship waves and ocean waves are conveniently given in compact complex notation. This makes it unnecessary, for example, to explicitly give the phase of the ship waves with respect to the ocean waves. The generalization of the single wave procedure to the multiple-wave random sea is discussed in detail. This includes the technique for selecting the frequencies and headings for modeling the random sea itself, the superposition of the ship waves due to each sea wave component, and the calculation of the ship and/or sea waves at any arbitrary point on the ocean surface. The formulation is given for the slopes as well as the elevations of these waves. The procedures required for adapting the transfer function and Kochin function output at the selected frequencies and headings of the Ship Motion Program SMP [4] to those modeling the random sea are discussed in some detail.

The preceding results are also generalized to the case of a twin hull, by essentially reflecting the Kochin functions for a single hull about the vertical plane of symmetry of the twin hull. The errors incurred by using the results of SMP, which is for a monohull, to generate waves for a twin hull are indicated.

Spatial realizations are then presented for the ship and/or sea wave elevations and slopes for four ship hulls in random seas corresponding to Sea States 2, 4, and 8. The spatial realizations are presented as three-dimensional plots, contour plots, and two-dimensional plots of wave elevations along a given line. Spatial realizations such as these do not appear to have been previously given. The report concludes with a summary of the principal findings.

Manuscript approved December 15, 1986.

2. FORMULATION FOR SINGLE EXCITING WAVE

2.1 Monohull Case

Adopting the usual assumption of linearized potential flow, the problem essentially consists of two parts: the evaluation of the potential flow on and near the ship hull and the extrapolation of this near field solution to obtain the far field waves.

The near field problem consists of finding a potential function ϕ which satisfies Laplace's equation, the free surface condition, the radiation condition of outward progressive waves at infinity, and the kinematic condition of no flow through the ship hull. In the commonly used Green's function approach, the procedure is to place a series of singularities on the hull surface which satisfy the first three conditions, and then to determine their strengths from the kinematic condition on the hull surface. In the present work, these strengths are calculated by using the Ship Motions Program SMP [4], which neglects longitudinal interactions between ship cross sections, thus reducing the three-dimensional problem to a series of simpler two-dimensional problems.

The coordinate system used in the *calculations* in SMP (and also used in the present work) is shown in Fig. 1. The origin lies on the undisturbed free surface, at the longitudinal center of gravity, and in the vertical plane of symmetry. The x-axis is directed forward, the y-axis to port, and the z-axis upwards. In this coordinate system, following and head seas correspond respectively to headings of 0 and 180 degrees. It should be noted that this coordinate system and sea heading convention do *not* correspond to those used for input and output in SMP.

To first order, the strengths of the sources obtained for the near field may also be used to obtain the far field waves [5]. However, the sources themselves must be changed from those for two dimensions, G_{2D}, to those for three dimensions, G_{3D}. In the present work, the resultant wave-making capability of the sources distributed over the hull surface is obtained in terms of the Kochin function, which represents a weighted integral of the source strengths over the hull surface.

Wehausen and Laitone [6] give the following asymptotic expression for the far field wave elevation ζ_j of the radiation wave due to an oscillation ξ_j of unit amplitude

$$\zeta_j \sim \mathrm{Re}\left[\frac{\omega}{g}\sqrt{\frac{k}{2\pi R}}\,\bar{H}_j(k,\theta)e^{i(kR+\omega t-\frac{\pi}{4})}\right]$$

$$= \mathrm{Re}\left[\frac{1}{4\pi}\frac{\omega}{g}\bar{H}_j\left(G^a_{3D}e^{i\omega t} = 2\pi\sqrt{\frac{2k}{\pi R}}e^{i(kR-\pi/4)}e^{i\omega t}\right)\right] \qquad (1)$$

where $j = 1,\ldots, 6$ denote the six modes of ship oscillation

$k = \dfrac{\omega^2}{g} = \dfrac{2\pi}{\lambda}$ is the wave number

ω is the circular frequency of the exciting wave

λ is the wavelength of the exciting wave

$R = \sqrt{x^2 + y^2}$ denotes the radius in the horizontal plane, measured from the origin shown in Fig. 1

$\theta = \tan^{-1}(y/x)$ is the direction in the horizontal plane, measured from the $x-$axis

$\bar{H}_j$ is the complex conjugate of the Kochin function H_j

G^a_{3D} is the asymptotic expression for the three-dimensional source potential at large R

The Kochin function H_j is given by

$$H_j(k,\theta) = -\iint_S \gamma_j(\xi,\eta,\zeta)e^{[k\zeta + ik(\xi\cos\theta + \eta\sin\theta)]}dS \qquad (2)$$

where γ_j is the hull surface distribution of singularity strengths calculated by SMP for the jth mode of ship oscillation; ξ,η,ζ are respectively the x,y,z coordinates of the source located on the hull surface. It is shown in [7,8] that at distances R greater than 0.3 λ, there is relatively little difference in the wave elevations calculated by the asympototic and complete formulas. In view of this, Eq. (1) is used to calculate ζ_j for $R \geq 0.3\lambda$. For $R < 0.3\lambda$, the coefficient $\sqrt{2k/\pi R}$ is simply set equal to $\sqrt{2k/\pi(0.3\lambda)}$; otherwise, $\zeta_j \to \infty$ as $R \to 0$.

The diffraction wave ζ_{R7} for an incident wave of unit amplitude is given by the sum of the vertical and lateral components ζ_{R7V} and ζ_{R7L}

$$\begin{aligned}\zeta_{R7} &= \zeta_{R7V} + \zeta_{R7L} \\ &= \mathrm{Re}\left[\frac{\omega}{g}\sqrt{\frac{k}{2\pi R}}\,(\bar{H}_{7V}(k,\theta,\beta) + \bar{H}_{7L}(k,\theta,\beta))\,e^{i(kR+\omega t-\pi/4)}\right]\end{aligned} \tag{3}$$

where β is the wave heading, $\bar{H}_{7V}$ and $\bar{H}_{7L}$ are respectively the complex conjugates of the symmetric (vertical plane) and antisymmetric (lateral plane) components of the diffraction Kochin functions H_{7V} and H_{7L}, which are evaluated from Eq. (2) with the singularity strengths

$$\gamma_{7V} = -\gamma_3 e^{-ik\xi\cos\beta} \tag{4a}$$

and

$$\gamma_{7L} = i\,\sin\beta\,\gamma_2 e^{-ik\xi\cos\beta} \tag{4b}$$

For the case where the ship oscillation is not of unit amplitude but is the response to a wave of amplitude α arriving with phase ϕ relative to the origin of the coordinate system, ζ_j in Eq. (1) must be multiplied by $\alpha e^{i\phi}$ and the transfer function $T_j(\omega,\beta)$, while ζ_{R7} must be multiplied by $\alpha e^{i\phi}$. In the present work, for the sake of computer programming convenience, the resultant of the radiation and diffraction waves, ζ_{RD}, is calculated by one single expression, as follows

$$\begin{aligned}\zeta_{RD}(\omega,\theta,\beta) &= \mathrm{Re}\left[\sum_{j=1}^{6}\alpha e^{i\phi}T_j(\omega,\beta)\,\zeta_j + \alpha e^{i\phi}(\zeta_{R7V}+\zeta_{R7L})\right] \\ &= \mathrm{Re}\left[\alpha e^{i\phi}\sum_{j=1}^{8}T_j(\omega,\beta)\,\zeta_j\right] = \mathrm{Re}\left[\sum_{j=1}^{8}\zeta_{RDj}\right]\end{aligned} \tag{5}$$

where $\zeta_7 = \zeta_{R7V}$

$\zeta_8 = \zeta_{R7L}$

$T_j(\omega,\beta) \equiv 1, \quad j = 7,8$

2.2 Twin Hull Case

In order to obtain an estimate of the wave patterns due to twin hull ships, the above formulation for monohulls has been generalized to approximately model the twin hull case. The procedure consists of summing the preceding expressions for the Kochin function, which are formulated for a monohull with vertical centerplane at $y = 0$, for two hulls with identical singularity distributions at $y = Y_1$, and $y = Y_2$. From Eq. (2), the resultant Kochin function H_{Tj} for the two hulls is given by the following sum for two monohulls

$$\begin{aligned}H_{Tj} &= H_j(y = Y_1) + H_j(y = Y_2) \\ &= H_j\,(e^{ikY_1\sin\theta} + e^{ikY_2\sin\theta}), \quad j = 1,2,\ldots 6,7,8\end{aligned} \tag{6}$$

For the particular case where the two hulls are symmetrically located $2Y$ apart about $y = 0$, H_{Tj} is given by

$$H_{Tj} = H_j (e^{-ikY\sin\theta} + e^{ikY\sin\theta}) = H_j\, 2\cos(kY\sin\theta) \tag{7}$$

The above procedure gives the wavemaking of two hulls which do not affect each other's motion and whose waves completely pass through the adjacent hull. In the actual twin hull case, there is both hydrodynamic and dynamic coupling between the motions of the two hulls and the channel between the two hulls is an area of mutual wave reflection.

In the case of roll motion, Jones [9] experimentally shows that the motions decrease with increased hull spacing, largely due to the increase in roll moment of inertia. For a three-fold increase in hull spacing, Jones obtains a two-fold decrease in the roll motion transfer function at the resonance frequency, with less difference at other frequencies. It is of interest to note that for a ship with zero forward speed, the case considered in the present work, there is little change with hull spacing in the vertical plane pitch and heave transfer functions. Thus, the present approach overestimates to some extent the roll motions but may be reasonably accurate for the vertical plane motions.

Lee [10] accounts for the hydrodynamic interaction between hulls, within the strip theory approach, by modifying the usual two-dimensional Green's function to consider the vertical center-plane between the two hulls as a plane of symmetry. This leads to a region of completely trapped waves between the two hulls. It is pointed out in [11,12] that this may lead to an exaggeration of the interaction effect since some of the waves inevitably leak out of the channel. It is pointed out in [11] that motions obtained by neglecting the hydrodynamic interaction, as is done in the present work, may lead to more accurate results.

Perhaps the most serious error in the wave patterns predicted by the present approach is in the channel area of trapped waves between the two hulls. It may be noted, however, that this is a near field region, which is not accurately modeled by the present far field approach.

3. WAVE ELEVATIONS AND SLOPES FOR RANDOM SEA CASE

3.1 Generation of Random Sea Elevations

Following the procedure outlined in [13,14], the random sea elevations $\zeta_{SE}(x,y,t)$ are approximated by a double sum over wave number k_m and wave heading μ_n of sinusoidal components, as follows

$$\zeta_{SE} = \mathrm{Re} \sum_{m=1}^{M} \sum_{n=1}^{N} \alpha_{mn} e^{i\phi_{mn}} e^{i[k_m(x\cos\mu_n + y\sin\mu_n) - \omega_m t]} = \mathrm{Re} \sum_{m=1}^{M} \sum_{n=1}^{N} \zeta_{SEmn} \tag{8}$$

where $\alpha_{mn} = \sqrt{2S(\omega_m)\Delta\omega}\,\sqrt{G(\mu_n)\Delta\mu} = \alpha_m \alpha_n$ (9a)

$S(\omega_m)$ is the value of the frequency spectrum at wave frequency ω_m

$G(\mu_n)$ is the value of the spreading function at wave heading μ_n, taken relative to the wind direction β_W

$\mu_n = \beta_n - \beta_W$ (9b)

β_n is the wave heading measured with respect to the x axis

$\Delta\omega$ and $\Delta\mu$ are increments in ω and μ

In the present approach, the following three widely used frequency spectra are considered: Pierson-Moskowitz, JONSWAP, and Neumann. The spreading function $G(\mu)$ is taken to be the commonly used cosine squared function

$$G(\mu) = \frac{2}{\pi} \cos^2 \mu \, , \, -\frac{\pi}{2} \leq \mu \leq \frac{\pi}{2} \tag{10}$$

It is shown in [13] that as few as five values of ω_m, chosen so as to give equal values of α_m, are sufficient to give wave amplitudes which approximate those of a random sea. In [14] it is suggested that 10 or more heading components are needed to give a visually random sea.

3.2 Ship Radiation and Diffraction Wave Elevations in a Random Sea

The resultant ship radiation and diffraction wave ζ_{SH} for the random sea case is obtained by summing the ship waves for a single incident wave, ζ_{RD} given in Eq. (5), for the above $M \times N$ sinusoidal components, resulting in the following triple sum

$$\zeta_{SH} = \mathrm{Re} \sum_{m=1}^{M} \sum_{n=1}^{N} \alpha_{mn} e^{i\phi_{mn}} \sum_{j=1}^{8} T_j \zeta_j = \mathrm{Re} \sum_{m=1}^{M} \sum_{n=1}^{N} \sum_{j=1}^{8} \zeta_{SHmnj} \tag{11}$$

The total of the ship and sea waves, ζ_T, is then simply given by

$$\begin{aligned} \zeta_T &= \zeta_{SE} + \zeta_{SH} \\ &= \mathrm{Re} \sum_{m=1}^{M} \sum_{n=1}^{N} \left(\zeta_{SEmn} + \sum_{j=1}^{8} \zeta_{SHmnj} \right) \end{aligned} \tag{12}$$

3.3 Wave Slopes

The preceding formulation for wave elevations may be conveniently used to obtain expressions for wave slopes. Taking x and y derivatives of the sea wave elevations given by Eq. (8) results in the following formulas for the x and y slopes, respectively ζ_{SEx} and ζ_{SEy}

$$\zeta_{SEx} = \mathrm{Re} \sum_{m=1}^{M} \sum_{n=1}^{N} ik_m \cos \mu_n \, \zeta_{SEmn} \tag{13}$$

$$\zeta_{SEy} = \mathrm{Re} \sum_{m=1}^{M} \sum_{n=1}^{N} ik_m \sin \mu_n \, \zeta_{SEmn} \tag{14}$$

Expressions for the x and y slopes of the ship waves are obtained by first taking the x and y derivatives of G_{3D}^a given in Eq. (1). Keeping only the lowest order term for large values of R, and further noting the definitions given for R and θ in Eq. (1), $\partial G_{3D}^a / \partial x$ and $\partial G_{3D}^a / \partial y$ are given by

$$\frac{\partial G_{3D}^a}{\partial x} \sim ik \frac{\partial R}{\partial x} G_{3D}^a = ik \cos\theta \, G_{3D}^a \tag{15}$$

$$\frac{\partial G_{3D}^a}{\partial y} \sim ik \frac{\partial R}{\partial y} G_{3D}^a = ik \sin\theta \, G_{3D}^a \tag{16}$$

From the summation given in Eq. (11), it follows that the x and y slopes of the resultant ship radiation and diffraction waves, ζ_{SHx} and ζ_{SHy}, are given by the following triple sums

$$\zeta_{SHx} = \mathrm{Re} \sum_{m=1}^{M} \sum_{n=1}^{N} \sum_{j=1}^{8} ik_m \cos\theta \, \zeta_{SHmnj} \tag{17}$$

$$\zeta_{SHy} = \mathrm{Re} \sum_{m=1}^{M} \sum_{n=1}^{N} \sum_{j=1}^{8} ik_m \sin\theta \, \zeta_{SHmnj} \tag{18}$$

The total of the ship and sea wave x and y slopes, ζ_{Tx} and ζ_{Ty}, are given by the following summations

$$\zeta_{Tx} = \zeta_{SEx} + \zeta_{SHx}$$

$$= \mathrm{Re} \sum_{m=1}^{M} \sum_{n=1}^{N} i \left[k_m \cos \mu_n \, \zeta_{SEmn} + k_m \cos \theta \sum_{J-1}^{8} \zeta_{SHmnj} \right] \tag{19}$$

$$\zeta_{Ty} = \zeta_{SEy} + \zeta_{SHy}$$

$$= \mathrm{Re} \sum_{m=1}^{M} \sum_{n=1}^{N} i \left[k_m \sin \mu_n \, \zeta_{SEmn} + k_m \sin \theta \sum_{j=1}^{8} \zeta_{SHmnj} \right] \tag{20}$$

4. COMPUTER IMPLEMENTATION OF METHOD

4.1 Computer Program SERDWAV

The formulation has been implemented in the form of computer program SERDWAV. The program accepts from one input file data on the speed and direction of the wind, the frequency spectrum to be used, the number of frequency components, and the types of waves to be calculated (ship, sea, or total of ship and sea; elevation, x slope, or y slope). In this same file are specified data for the rectangular grid over which the waves are calculated: its origin, and the number and spacing of the points along the (x',y') axes, which are inclined at angle α to the (x,y) system (see Fig. 2). In the case of a twin hull, this file also gives the lateral offsets Y_1 and Y_2 of the vertical centerplanes of the two hulls. As a second input file, the program accepts the Kochin functions $H_j(\omega,\theta,\beta)$ and transfer functions $T_j(\omega,\beta)$ calculated by SMP [4].

The program then performs the calculations for the wave elevations and slopes given by Eqs. (8)-(20). In the case of a twin hull, the Kochin functions H_j are modified according to Eq. (6). The calculated waves are saved as an output plot file from which three-dimensional, two-dimensional or contour plots may be generated. Examples of these plots are given in the following chapter.

4.2 Adaptation of Formulation to SMP Results

Program SMP calculates the functions H_j and T_j for 30 discrete values of ω between 0.2 and 2.4 rad/sec, and 13 equally spaced values of θ and β between 0 and 180 degrees. Thus, it is of interest to describe the procedure used to model the general case of values of ω, β, and θ which may not coincide with, or fall outside the range of, the SMP results.

4.2.1 Procedure for wave frequencies ω

In order to more accurately model the lower sea states, where the higher ω's are of interest, the two highest frequencies calculated by SMP were changed from 2.2 and 2.4 to 2.4 and 2.8 rad/sec, respectively. This essentially consisted of changing one DATA statement in SMP. The actual values of ω (and the corresponding values of wavenumber k) appearing explicitly in Eqs. (8)-(20) are retained. On the other hand, the values of H_j and T_j are approximated by those corresponding to the SMP values of ω which come closest to the actual values.

4.2.2 Procedure for wave headings μ and β

Since the results of [14] indicate that a minimum of approximately 10 wave headings are required to give visually random seas, it was decided to simply adopt the 13 equally spaced headings between 0 and 180 degrees, as used by SMP. Noting that the energy of the wind is spread 90 degrees on either side of the wind direction (see Eq. (10)), the SMP formulation is most conveniently

used when the wind direction is 90 degrees, i.e., in this case the wave headings of interest are simply the 0 to 180 degree cases considered by SMP. For other wind directions, however, Fig. 3 shows that negative values of β are involved. In these cases, use is made of the fact that for the vertical modes (j = 1,3,5,7) $T_j(\omega,-\beta) \equiv T_j(\omega,\beta)$, while for the lateral modes (j=2,4,6,8) $T_j(\omega,-\beta) \equiv -T_j(\omega,\beta)$. These relations are conveniently summarized by the following equation

$$T_j(\omega,-\beta) = (-1)^{j+1} T_j(\omega,\beta), \quad j = 1,2,\ldots,7,8 \tag{21}$$

Figure 3 also shows that when the wind direction β_W is not 90 degrees, not all 13 values of β considered by SMP are used. In these cases, the appearance of negative values of β essentially means the double use of the values of H_j and T_j corresponding to that β. For example, for β_W = 0 degrees, only values of H_j and T_j lying between 0 and 90 degrees are needed. Thus, a selection and rearrangement of the SMP output values of H_j and T_j are required for $\beta_W \neq$ 90 degrees.

Once the proper values of ω and β have been selected, the wave amplitudes α_{mn} can be conveniently evaluated by Eq. (9a), where μ, the wave heading relative to the wind direction, is given in terms of β and β_W by Eq. (9b).

4.2.3 Procedure for Arbitrary Values of θ

The Kochin functions H_j are used as follows to calculate wave elevations and slopes at field points (x,y) for cases where the value of θ, defined in Eq. (1), does not correspond exactly to one of the 13 evenly spaced values between 0 and 180 degrees considered by SMP. For positive values of θ, i.e., the field point has a positive value of y, the value of H_j is obtained simply by linear interpolation between the two SMP values of H_j which bracket the given value of θ. For negative values of θ, $H_j(-\theta)$ is related to $H_j(\theta)$ by noting that the ship waves are symmetrical with respect to θ for the vertical modes (j=1,3,5,7) and antisymmetric for the lateral modes, i.e.,

$$H_j(-\theta) = (-1)^{j+1} H_j(\theta), \quad j = 1,2,\ldots,7,8 \tag{22}$$

5. CALCULATED WAVE PATTERNS

5.1 Choice of Ship Hulls

Program SERDWAV was used to calculate sample wave patterns for four hulls. Principal geometric dimensions of the hulls are given in Table 1. The table gives the length L, beam at the free surface B, draft H, and (in the case of the twin hull) spacing 2Y between the vertical centerplanes of the hulls.

Figures 4 and 5 respectively show the section contours of the DE1006 and CVA59 hulls while Fig. 6 shows top and side views of the TAGOSTW twin hull. The DE1006 is a destroyer type hull, the CVA59 represents an aircraft carrier, and the TAGOSTW is a geometrically simplified version of the small-waterplane-area twin hull (SWATH) T-AGOS described in [15]. The TAGOSMH represents the monohull version of the TAGOSTW.

5.2 Choice of Sea States

Most of the runs were made using a wind speed of 18 knots, which represents Sea State 4. The sea is represented by five frequencies chosen so as to give equal wave amplitudes α_m, and 13 wave headings equally spaced 90 degrees on either side of the wind direction, in accordance with Eq. (10). To give an indication of the variation of the wind speed on the wave patterns, runs were also made for wind speeds of 12 and 42 knots, which correspond respectively to Sea States 2 and 8. For these three wind speeds, Table 2 shows the five chosen values of ω, the corresponding wavelength λ, and the index number of the frequency in SMP which is closest to the chosen ω. For the 18-knot case,

Table 2 shows that the shortest wavelength of 58 ft is comparable to the draft or beam of most of the hulls, while the longest wavelength of 302 ft approximates the length of most of the hulls. For most runs, the wind wave direction β_W was fixed at 45 degrees, i.e. quartering seas. Some runs were also made for β_W equal to 0 and 90 degrees, i.e., following and beam seas.

5.3 Plots of Wave Patterns

For the three-dimensional and contour plots, wave elevations and slopes were calculated over a square $x-y$ grid, with $0 \leq x, y \leq 2\lambda_M$, where λ_M is the value of the largest wavelength λ shown in Table 2 for a given wind speed. Thus, $2\,\lambda_M$ is equal to 268, 604, and 3,306 ft for wind speeds of 12, 18, and 42 knots, respectively. The computation square was subdivided into 60 × 60 cells, each with a length equal to $\lambda_M/30$, thus modeling two cycles of the maximum wavelength. Since Table 2 shows that the minimum value of λ, λ_m, is approximately equal to $\lambda_M/5$, this means that the shortest wavelength was modeled by approximately six points. The two-dimensional plots were calculated for the 18-knot case along an axis x' inclined at angle α to the x axis for 101 points spaced 10 ft apart, i.e., $0 \leq x' \leq 1000$ ft.

5.3.1 Three-Dimensional Plots

Figures 7a - 7c show ambient wave elevations for wind speed V equal to 18 knots (Sea State 4) for wind direction $\beta_W = 0$, 45, and 90 degrees, respectively. Figures 7d - 7e respectively show the x and y wave slopes for $V = 18$ knots and $\beta_W = 45$ degrees. Figures 8a - 8d show the resultant ship radiation and diffraction waves for the four hulls for $V = 18$ knots and $\beta_W = 45$ degrees. Figures 9a - 9d show the superposition of the ship and ambient waves for the four hulls for the same sea conditions.

Figures 7a - 7c show that the sea crests tend to align perpendicular to the wind direction. This is due to the fact that even though the wind energy is spread over a range of directions, the principal energy is still centered at the wind direction, see Eq. (10). Figures 7d and 7e show that the crests of the x and y wave slopes tend to align perpendicular to the x and y axes, respectively.

Figure 8 shows that the ship waves tend to have larger amplitudes along the x-axis. This is largely due to the fact that the length of the ship is much larger than its width, resulting in greater diffraction of the waves traveling along the length of the ship. Comparison of Figs. 8d and 8e shows that the presence of the second hull gives only a small change in the wave pattern compared to that of the monohull.

Comparison of the plot of the ambient sea shown in Fig. 7b with the superposed sea and ship waves shown in Fig. 9 shows that for the three smallest hulls the presence of the hull makes a relatively small change to the ambient wave pattern. The exception occurs for the CVA59 which makes a large change to the ambient wave pattern. This is due to its large size which gives rise to resultant large diffraction waves.

5.3.2 Contour Plots

A different view of the wave pattern may be obtained by plotting contours of equal wave elevation. Figure 10 shows contours of the ambient sea waves for the following cases:

a. $V = 18$ knots, $\beta_W = 0$ deg
b. $V = 18$ knots, $\beta_W = 45$ deg
c. $V = 18$ knots, $\beta_W = 90$ deg
d. $V = 12$ knots, $\beta_W = 45$ deg
e. $V = 42$ knots, $\beta_W = 45$ deg

Figures 11a - d show the contour lines of the superposed ship and ambient waves for the four hulls for the wind conditions given in Fig. 10b. Figures 11e and f respectively show the superposed contour lines for the DE1006 for the wind conditions given in Figs. 10d and e.

As was previously noticed in the case of the three-dimensional plots, Fig. 10 clearly shows that the contour lines tend to align perpendicular to the wind direction. In the absence of any energy spread, the contours would, of course, be straight lines exactly perpendicular to the wind direction.

Figures 10b, d, and e show the interesting feature that the contour lines for a given value of β_W(= 45 deg), the ambient wave contour lines for different wind speeds are quite similar. This is largely a consequence of the size of the computation grid scaled to be equal to twice the maximum wavelength, as well as the similar ratios between the five component wavelengths which are selected to model the sea (see Table 2).

Figures 11a-d again show that for the three smallest hulls, the presence of the hull in a 18-knot sea makes a relatively small change to the contour lines of the ambient waves alone, shown in Fig. 10b. On the other hand, as previously noted in the three-dimensional plots, the presence of the 990-ft CVA59 makes a large change to the contour lines. This effect of ship size relative to ambient wavelengths on the resultant perturbation to the ambient waves is also clearly illustrated in Figs. 11e and f. Figure 11e shows that the DE1006 hull makes a large change to the contours of the short-wavelength 12-knot sea shown in Fig. 10d. On the other hand, Fig. 11f shows that this hull hardly makes any changes to the contours of the long-wavelength 42-knot sea, shown in Fig. 10e.

5.3.3 Two-Dimensional Plots

Figures 12 a-c show curves of the ambient waves and superposed ship and ambient waves for the DE1006 in the presence of a V = 18 knot, β_W = 0 deg ambient sea along an axis x' inclined respectively at 0, 45, and 90 degrees to the x axis. Figures 12d-f and 12g-i show corresponding results for β_W = 45 and 90 deg, respectively. Figures 12j-l show curves of the ambient and superposed waves along the x axis (α = 0 deg) for the CVA59 for V = 18 knots and β_W = 0, 45, and 90 deg, respectively.

As previously noted in the three-dimensional plots, Fig. 12 shows that the largest ship waves occur along the x axis, α = 0 deg, due to the large diffraction of waves in this direction. For the DE1006, Figs. 12a, d, and g show that the ship waves are relatively small but still noticeable at x = 1000 ft. The figure shows that the ship waves for α = 45 and 90 deg are smaller than those for α = 0 deg. Figures 12c, f, and i show the expected trend that the ship waves for α = 90 deg increase as the wind direction shifts from 0 to 90 deg. Thus, Figs. 12g-i show that for β_W = 90 deg, the ship waves for all values of α are still noticeable (relative to the ambient waves) at x' = 1000 ft.

Figures 12j-l show the much larger magnitude of the ship waves in the case of the CVA59. For example, at x = 1000 ft, the ship waves are still larger than the ambient waves.

6. SUMMARY

This report has discussed in detail the procedure for generating spatial realizations of the far field ship radiation and diffraction waves in the presence of random ambient sea waves. The procedure essentially consists of generalizing a previously described technique for obtaining the ship wave pattern due to a single incident wave, using the Kochin function approach, to the multiple waves of a random sea. The random sea waves are expressed as a double sum over frequency and heading of randomly phased sinusoidal components. The ship waves are expressed as a triple sum over eight ship wave modes and the above frequencies and headings. The eight wave modes consist of radiation wave modes due to the six oscillatory motions of the ship, and the vertical and lateral components of the diffraction wave due to scattering by the hull surface. It is shown that by a combination of interpolation, and use of the symmetry and antisymmetry properties of the ship wave modes, the discrete

set of Kochin functions and motion transfer functions output by the Ship Motion Program (SMP) may be used to calculate ship wave elevations for random sea waves at arbitrary field point locations.

It is shown that the horizontal x and y slopes of the waves may be conveniently obtained from the expression for wave elevation by multiplication by the wavenumbers in the x and y directions, respectively. The formulation for a monohull is also generalized to the twin hull case by considering the vertical plane midway between the hulls as a plane of symmetry. It is shown that this approach may qualitatively give the wave pattern for field points outside the channel area between the two hulls.

Sea and ship waves are presented for four ship hulls in the presence of various ambient seas in the form of three-dimensional, two-dimensional, and contour plots. Three of the hulls are 250 to 308 feet long, while the fourth hull is the 990-ft aircraft carrier CVA59. The plots for the sea waves show that their contours tend to be aligned perpendicular to the wind direction. The ship radiation and diffraction waves are largest along x, the direction parallel to the ship longitudinal axis. The ship waves along y, the horizontal direction perpendicular to x, increase as the wind direction shifts from x to y. In a Sea State 4, the presence of the 250 and 308 ft ships makes a moderately small change to the ambient waves, while the 990-ft CVA59 makes a large change. Similarly, relative to the sea waves, the ship waves due to the 308-ft DE1006 are large in a Sea State 2 and nearly imperceptible in a Sea State 8. The presence of a second hull gives a small, though perceptible, change to the wave pattern of a monohull.

7. ACKNOWLEDGMENT

This study was conducted as part of a research program in marine hydrodynamics supported by the Naval Research Laboratory.

8. REFERENCES

1. Wang, H.T., "Calculation of Far Field Radiation and Diffraction Wave Patterns Using the Kochin Function Approach for a Series of Ship Hulls," NRL Memorandum Report 5822, September 1986. (AD-A173448)

2. Hammond, R.R., Buntzen, R.R., and Floren, E.E., "Using Ship Wake Patterns to Evaluate SAR Ocean Wave Imaging Mechanisms," Naval Ocean Systems Center (NOSC) Technical Report 978, February 1985. (AD-A154633)

3. Barnell, A. and Noblesse, F., "Far Field Features of the Kelvin Wake," *Sixteenth ONR Symposium on Naval Hydrodynamics*, University of California at Berkeley, July 1986. Also DTNSRDC-86/054, September 1986. (AD-A172288)

4. Meyers, W.G., Applebee, T.R., and Baitis, A.E.," User's Manual for the Standard Ship Motion Program, SMP," DTNSRDC Report SPD-0936-01, September 1981.

5. Newman, J.N., *Marine Hydrodynamics*, MIT Press, Cambridge, Massachusetts, 1978.

6. Wehausen, J.V. and Laitone, E.V., "Surface Waves," *Encyclopedia of Physics*, Vol. 9, Springer-Verlag, Berlin, pp. 446-778, 1960.

7. Marnyanskii, I.A., "Diffraction of Waves Around a Submerged Vertical Plate," *Prikladnaya Matematika i Mekhanika*, Vol. 18, No. 2, pp. 233-238, 1954 (in Russian).

8. Liu, H.C., "Über die Entstehung von Ringwellen an einer Flüssigkeitsoberfläche durch unter dieser gelegene, kugelige periodische Quellensysteme," *Zeitschrift für Angewandte Mathematik und Mechanik*, Vol. 32, No. 7, pp. 211-226, July 1952.

9. Jones, H.D., "Catamaran Motion Predictions in Regular Waves," NSRDC Report 3700, January 1972. (AD-737204)

10. Lee, C.M., "Theoretical Prediction of Motion of Small-Waterplane-Area, Twin-Hull (SWATH) Ships in Waves," DTNSRDC Report 76-0046, December 1976. (AD-A033912)

11. Hadler, J.B., Lee, C.M., Birmingham, J.T., and Jones, H.D., "Ocean Catamaran Seakeeping Design, Based on the Experiences of USNS Hayes," *Transactions of the Society of Naval Architects and Marine Engines*, Vol. 82, pp. 126-161, November 1974.

12. Wang, S. and Wahab, R., "Heaving Oscillations of Twin Cylinders in a Free Surface," *Journal of Ship Research*, Vol. 15, No. 1, pp. 33-48, March 1971.

13. Wang, H.T., "Temporal and Spatial Simulations of Random Ocean Waves," *Proceedings of the Fourth Offshore Mechanics and Arctic Engineering Symposium*, Vol. 1, pp. 72-80, February 1985.

14. Wang, H.T., "Simulations of Velocities and Slopes of Random Ocean Waves," *Proceedings of the Fifth Offshore Mechanics and Arctic Engineering Symposium*, Vol. 1, pp. 382-389, April 1986.

15. Salvesen, N., von Kerczek, C.H., Scragg, C.A., Cressy, C.P., and Meinhold, M.J., "Hydro-Numeric Design of SWATH Ships," *Transactions of the Society of Naval Architects and Marine Engineers*, Vol. 93, pp. 325-346, November 1985.

Table 1 — Hull Geometric Characteristics

Ship Hull	L(ft)	B(ft)	H(ft)	2Y(ft)
1. DE1006	308.	35.9	12.1	—
2. CVA59	990.	129.3	35.8	—
3. TAGOSTW	250.	7.0	24.3	80.
4. TAGOSMH	250.	7.0	24.3	—

Table 2 — Wave Components
for Sea States 2, 4, and 8

ω(rad/sec)	λ(ft)	SMP #
Sea State 2, V=12 knots		
1.229	134	23
1.433	99	25
1.635	76	26
1.922	55	28
2.774	26	30
Sea State 4, V=18 knots		
0.818	302	17
0.956	221	20
1.092	170	22
1.285	123	24
1.874	58	27
Sea State 8, V=42 knots		
0.349	1,653	4
0.410	1,204	5
0.468	924	8
0.551	666	11
0.806	312	17

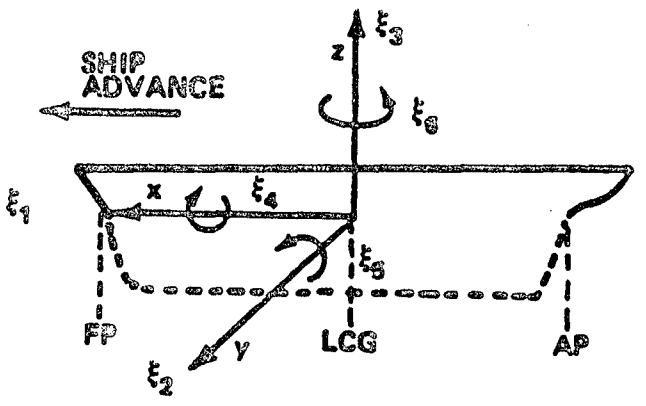

ξ_1 = SURGE
ξ_2 = SWAY
ξ_3 = HEAVE
ξ_4 = ROLL
ξ_5 = PITCH
ξ_6 = YAW

Figure 1 — Definition of coordinate system and modes of ship oscillation

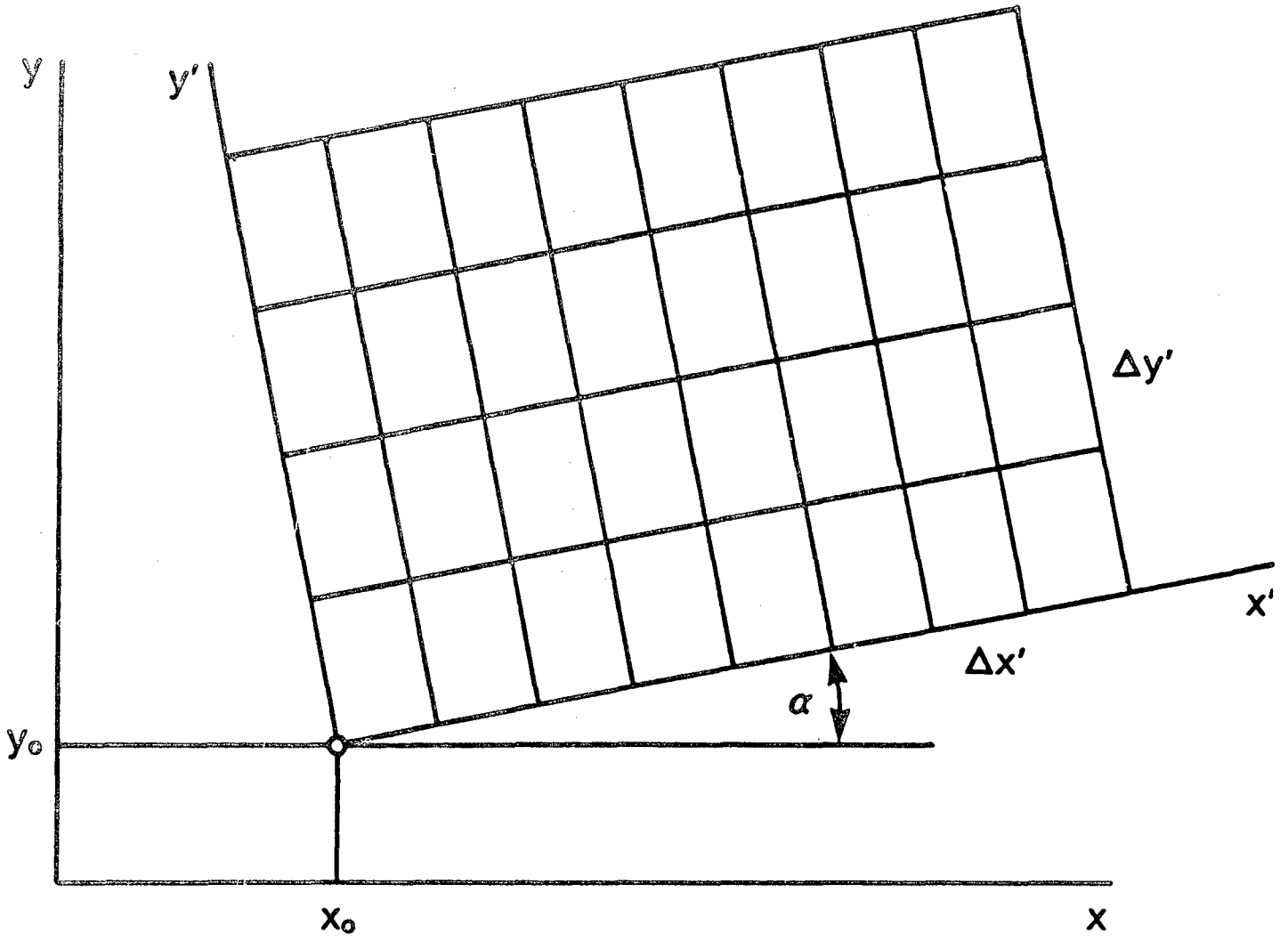

Figure 2 — Definition of calculation grid

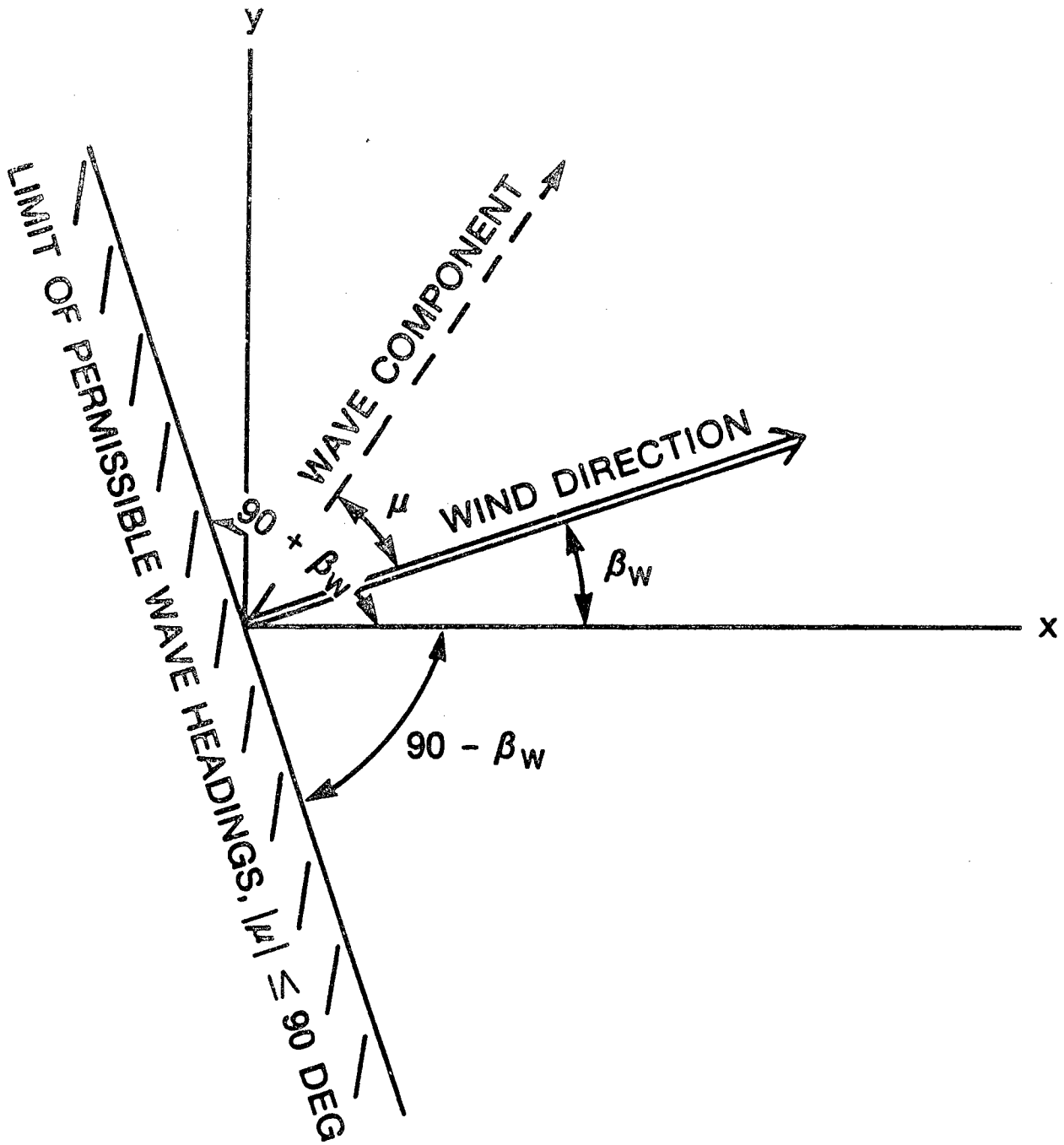

Figure 3 — Relation of sea wave headings to wind direction

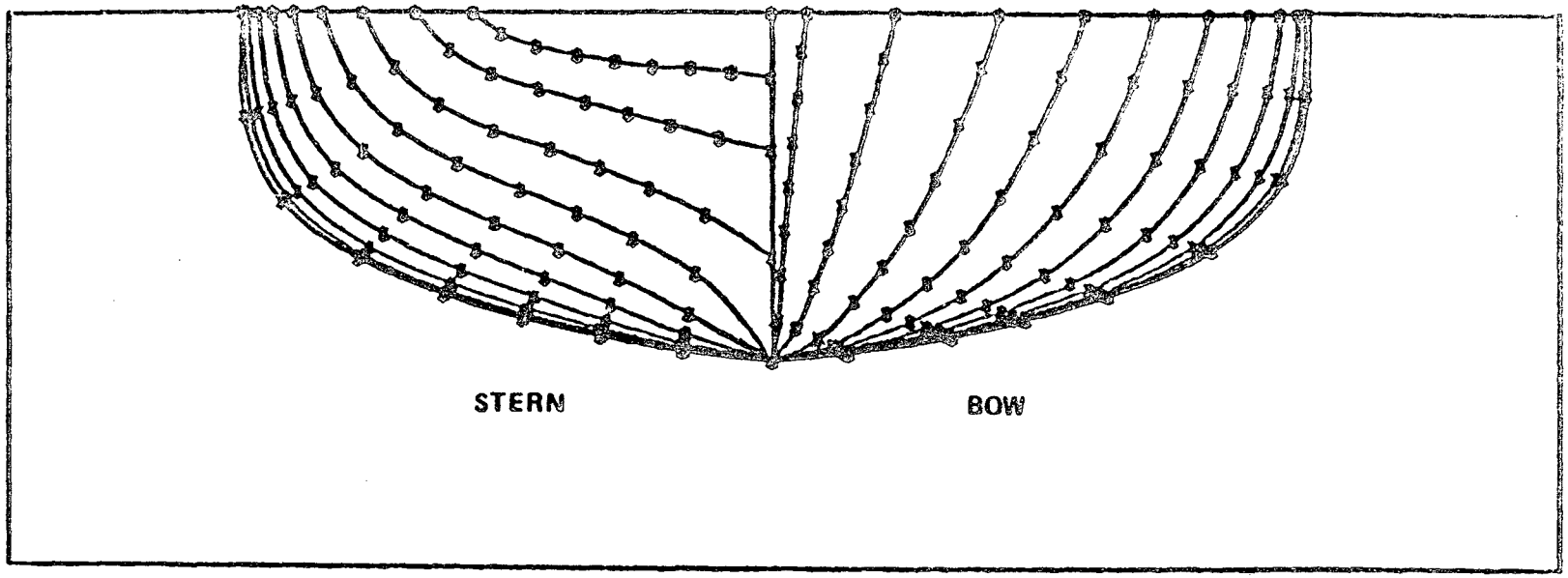

Figure 4 — Section contours for destroyer hull form DE1006

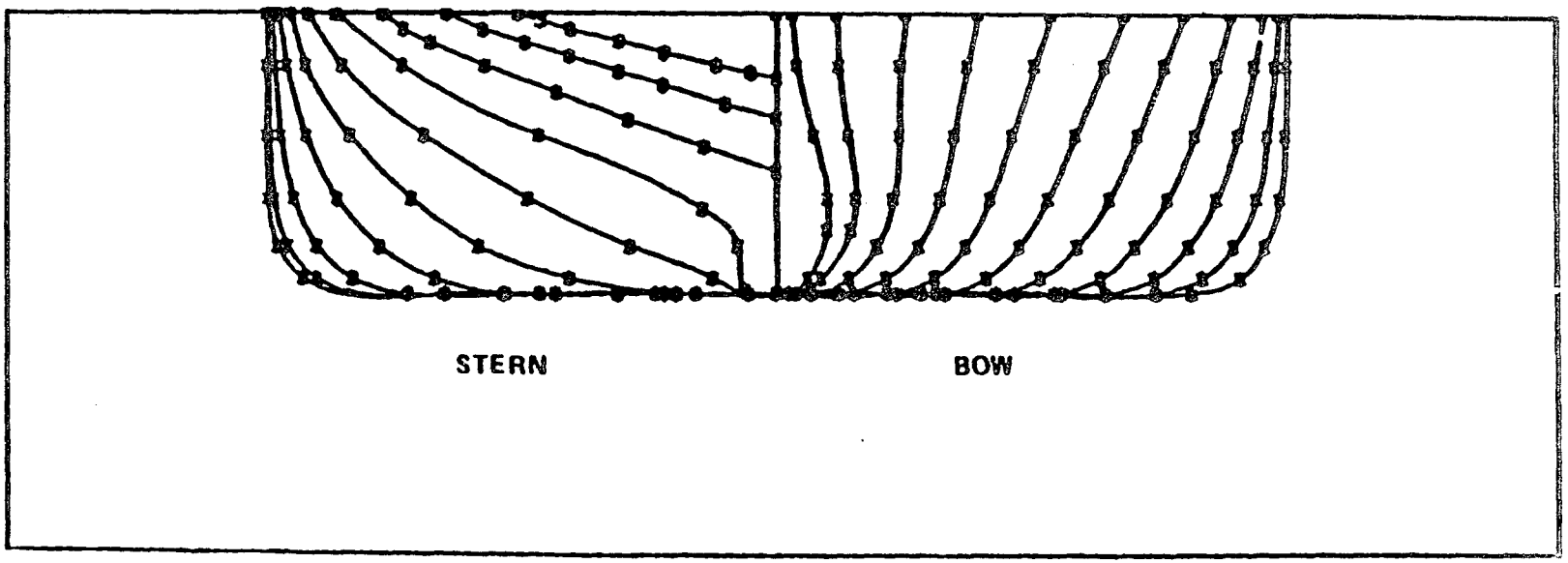

Figure 5 — Section contours for carrier hull form CVA59

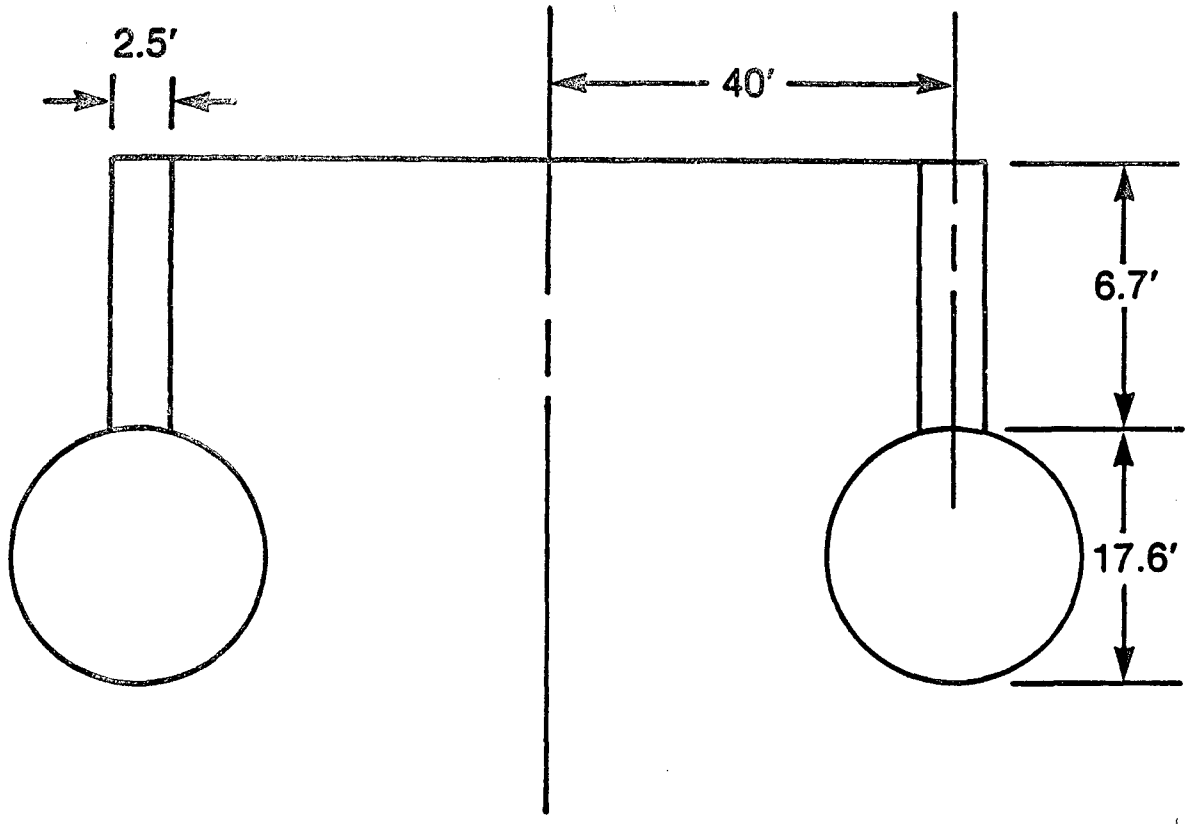

FRONT VIEW OF TAGOSTW TWIN HULL

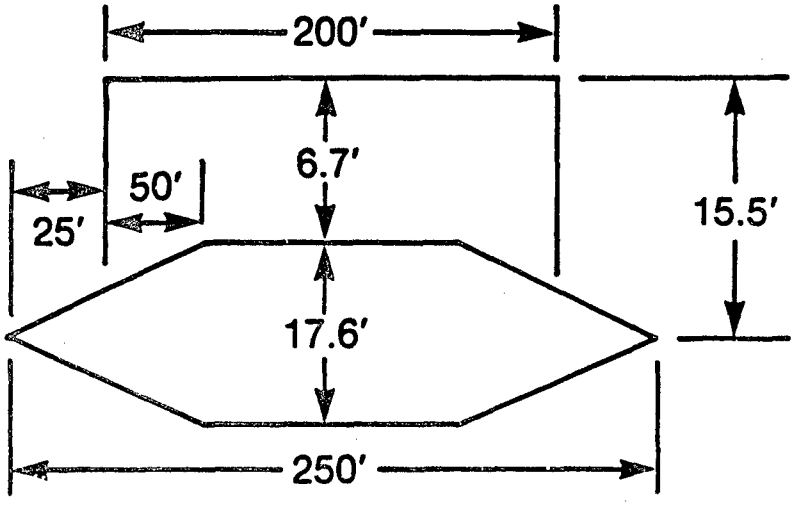

SIDE VIEW OF TAGOSTW TWIN HULL

Figure 6 — Geometry of small waterplane twin hull TAGOSTW

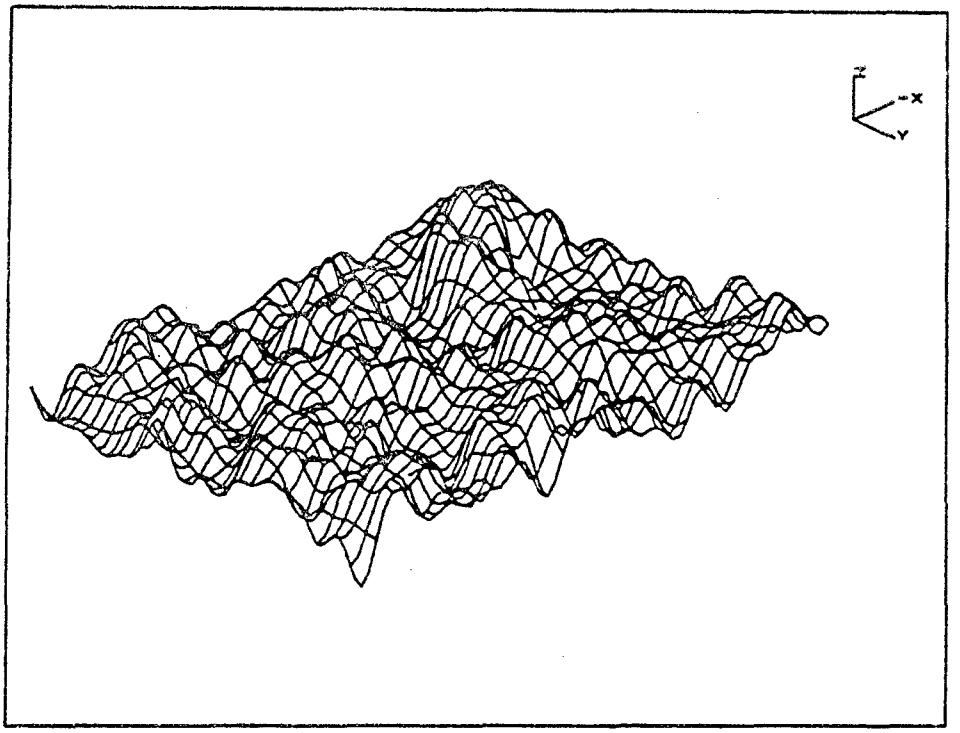

(a) Elevation, V = 18 knots, β_W = 0 deg

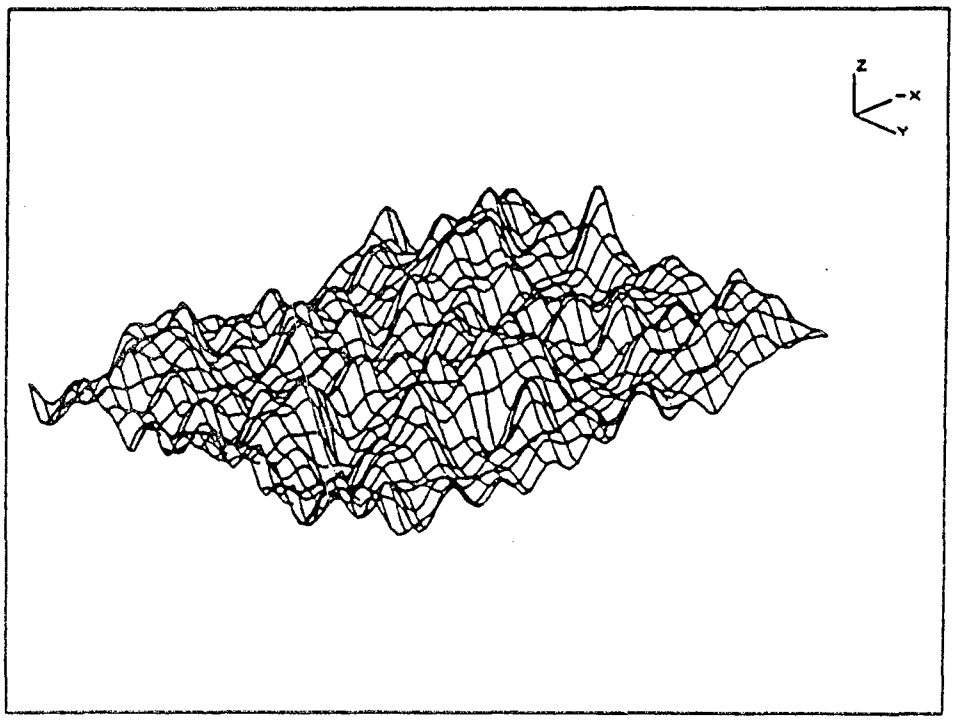

(b) Elevation, V = 18 knots, β_W = 45 deg

Figure 7 — Three-dimensional plots of ambient wave elevations and slopes

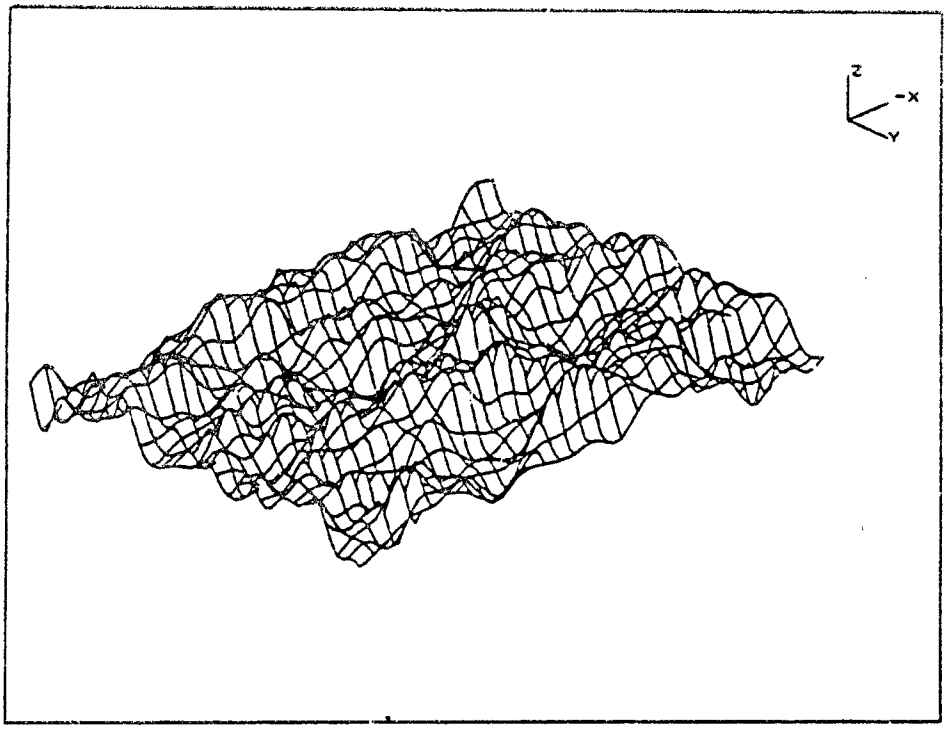

(c) Elevation, V=18 knots, β_W = 90 deg

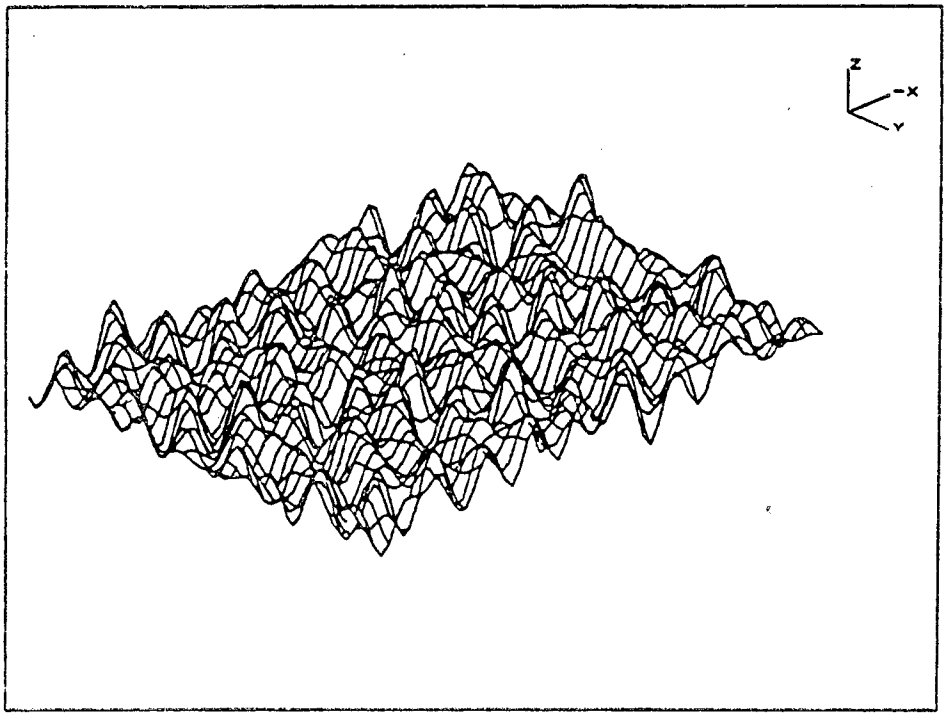

(d) x-slope, V=18 knots, β_W = 45 deg

Fig. 7 (Continued) — Three-dimensional plots of ambient wave elevations and slopes

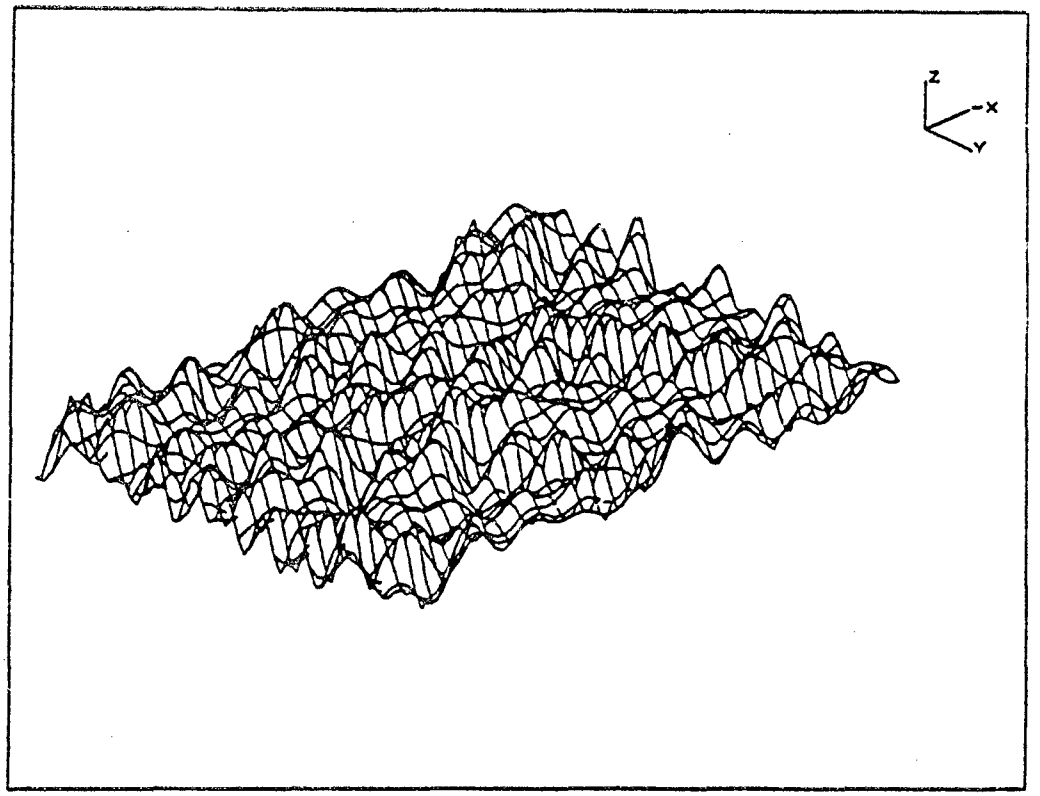

(e) y-slope, V = 18 knots, β_W = 45 deg

Fig. 7 (Continued) — Three-dimensional plots of ambient wave elevations and slopes

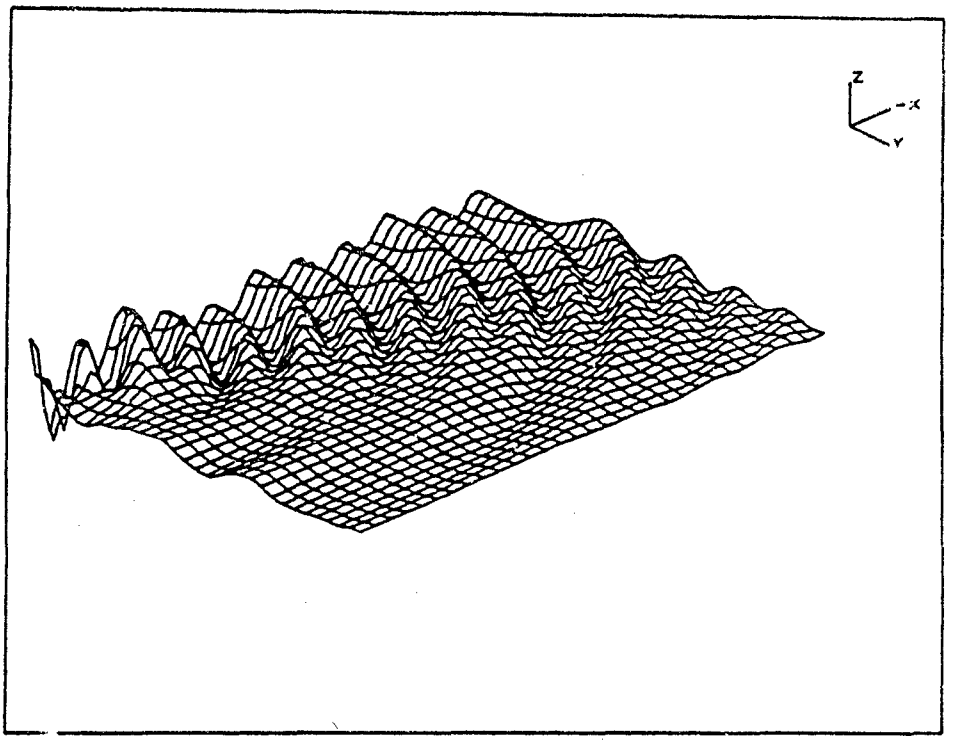

(a) Destroyer hull form DE1006

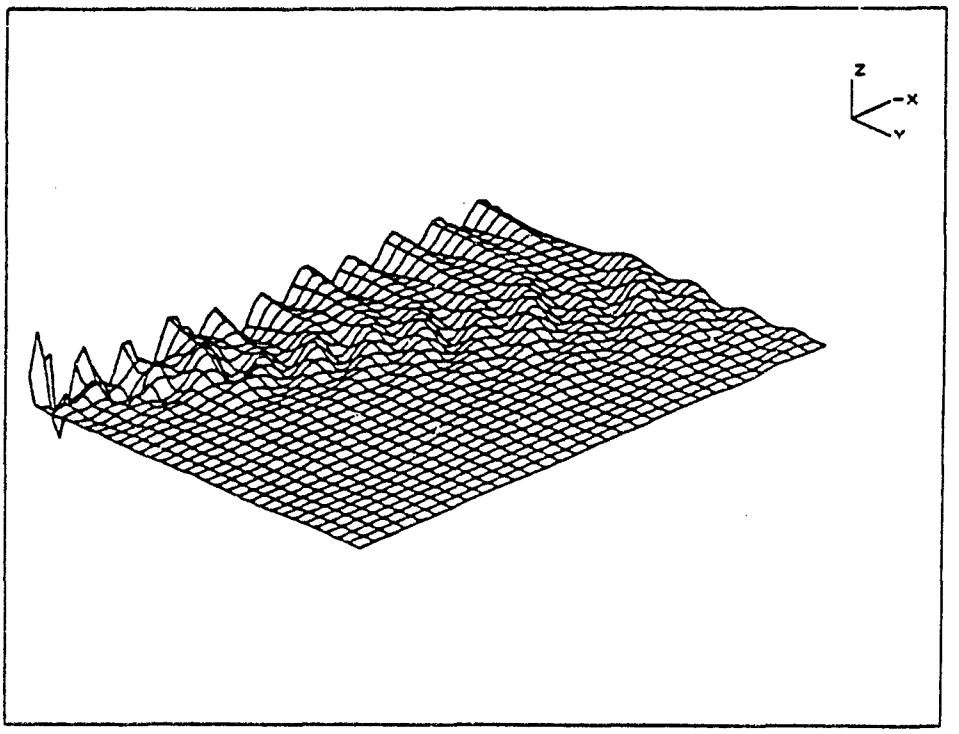

(b) Carrier hull form CVA59

Figure 8 — Ship radiation and diffraction waves for V = 18 knots, β_W = 45 deg

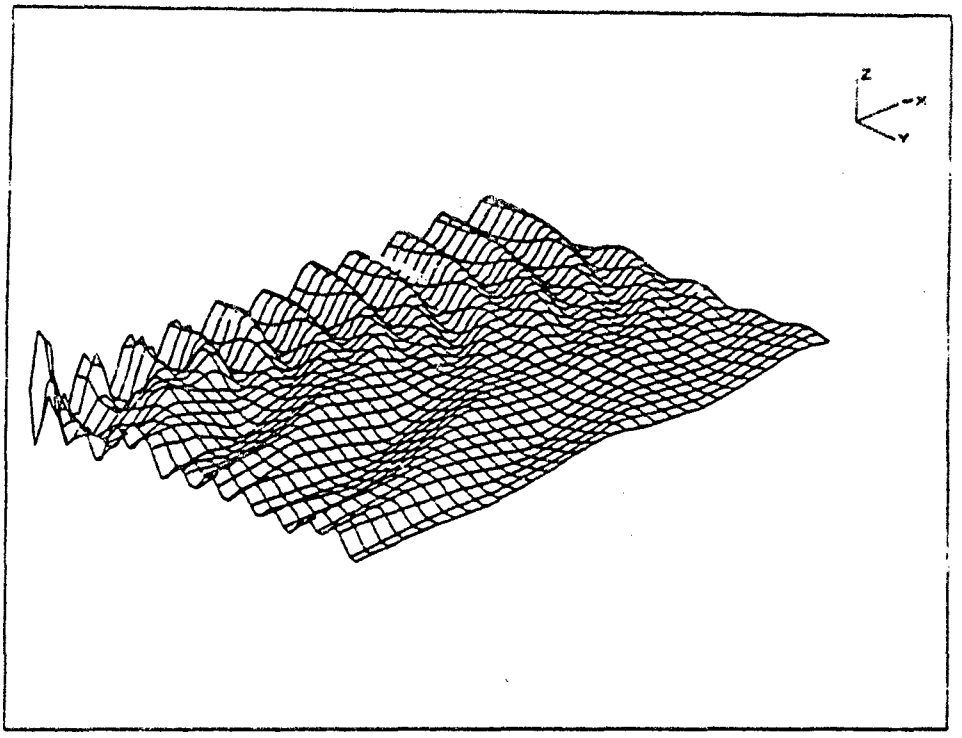

(c) Small waterplane area twin hull TAGOSTW

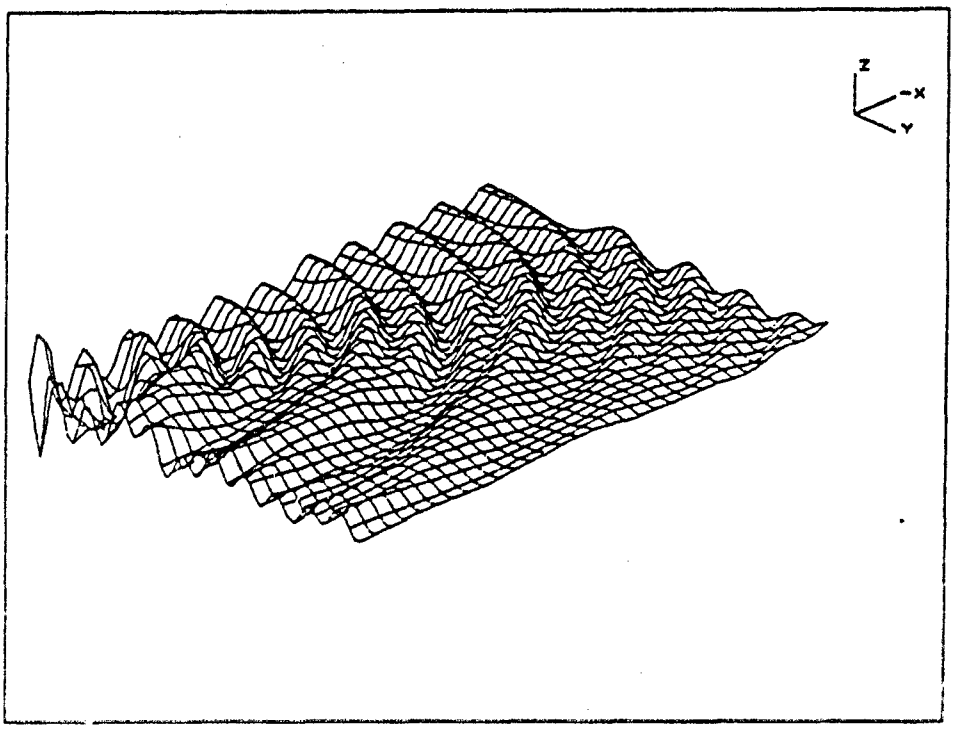

(d) Small waterplane area monohull TAGOSMH

Fig. 8 (Continued) — Ship radiation and diffraction waves for V = 18 knots, β_W = 45 deg

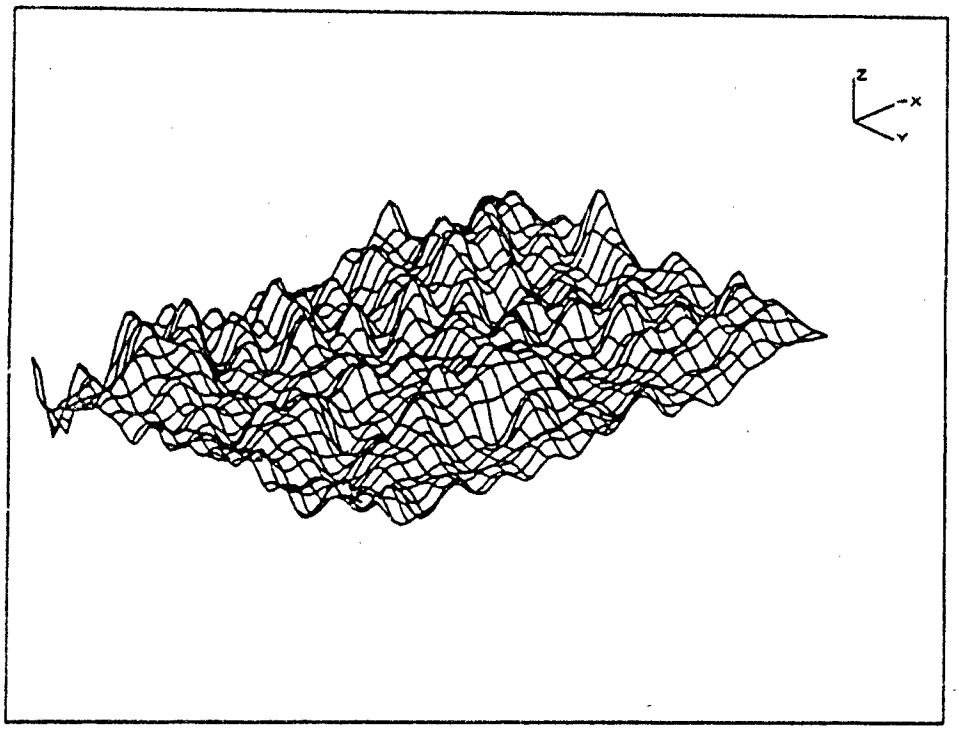

(a) Destroyer hull form DE1006

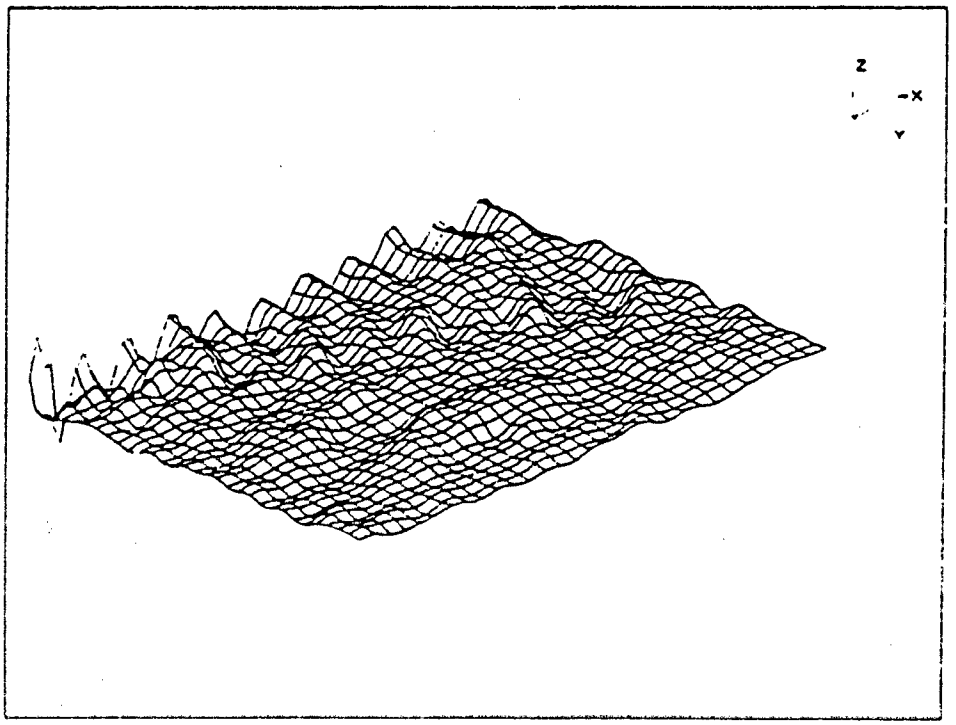

(b) Carrier hull form CVA59

Figure 9 — Superposed ship and ambient waves for V = 18 knots, β_W = 45 deg

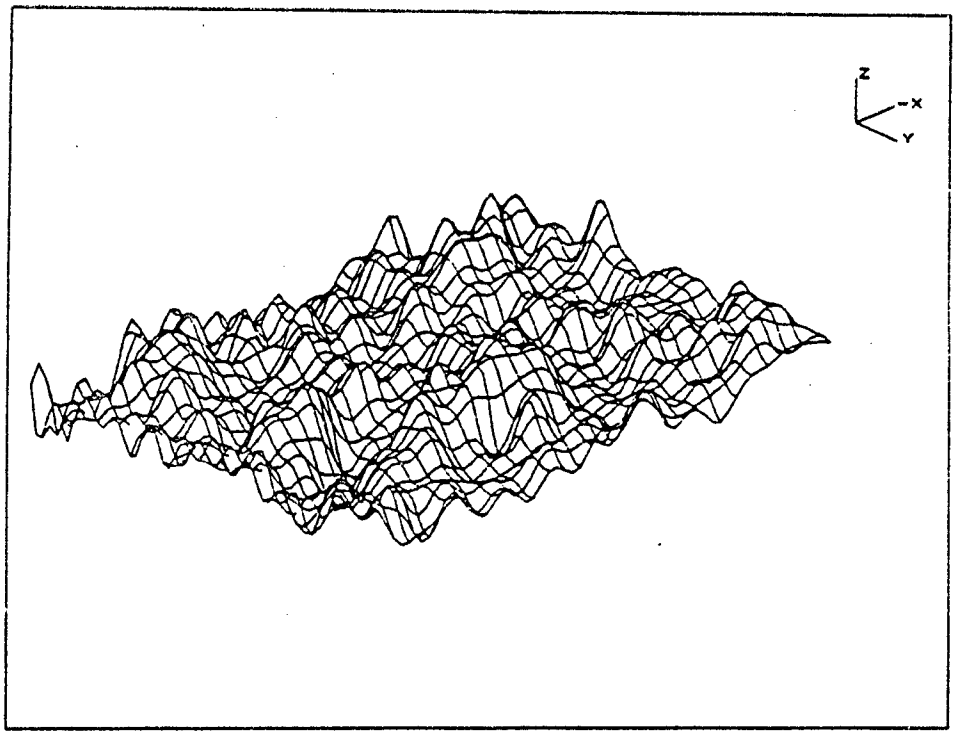

(c) Small waterplane area twin hull TAGOSTW

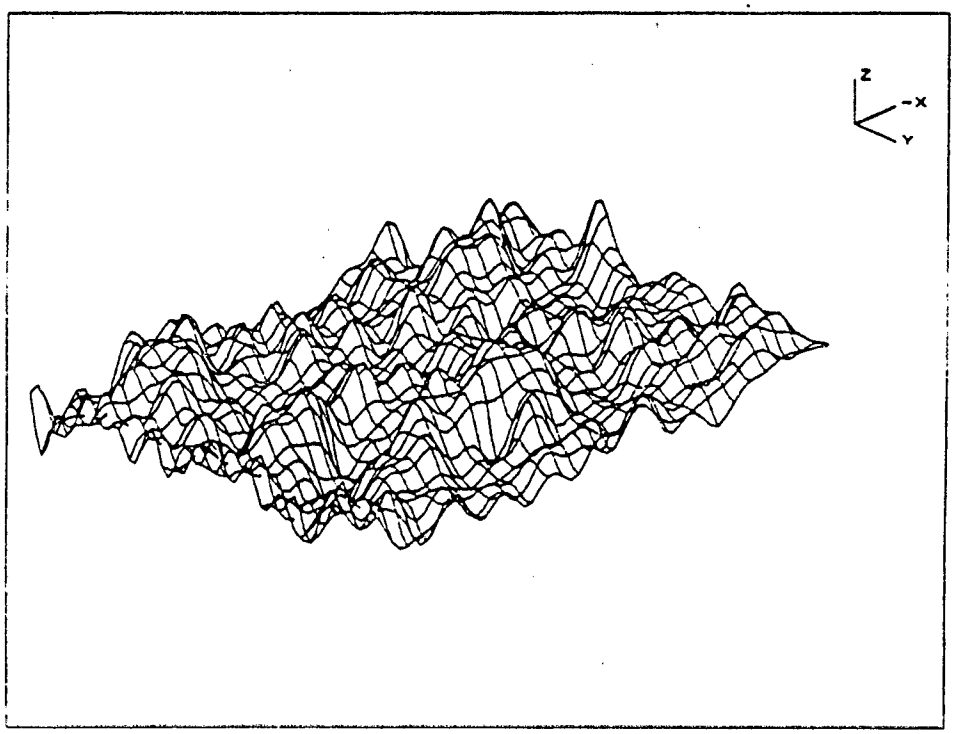

(d) Small waterplane area monohull TAGOSMH

Fig. 9 (Continued, — Superposed ship and ambient waves for V = 18 knots, β_W = 45 deg

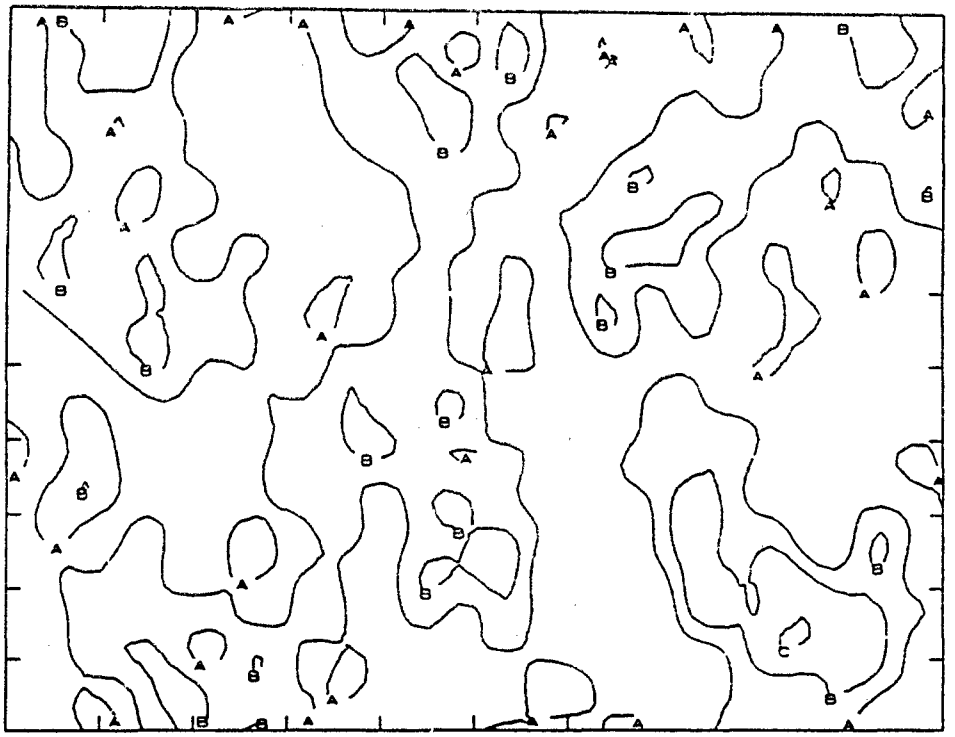

(a) V=18 knots, β_W = 0 deg

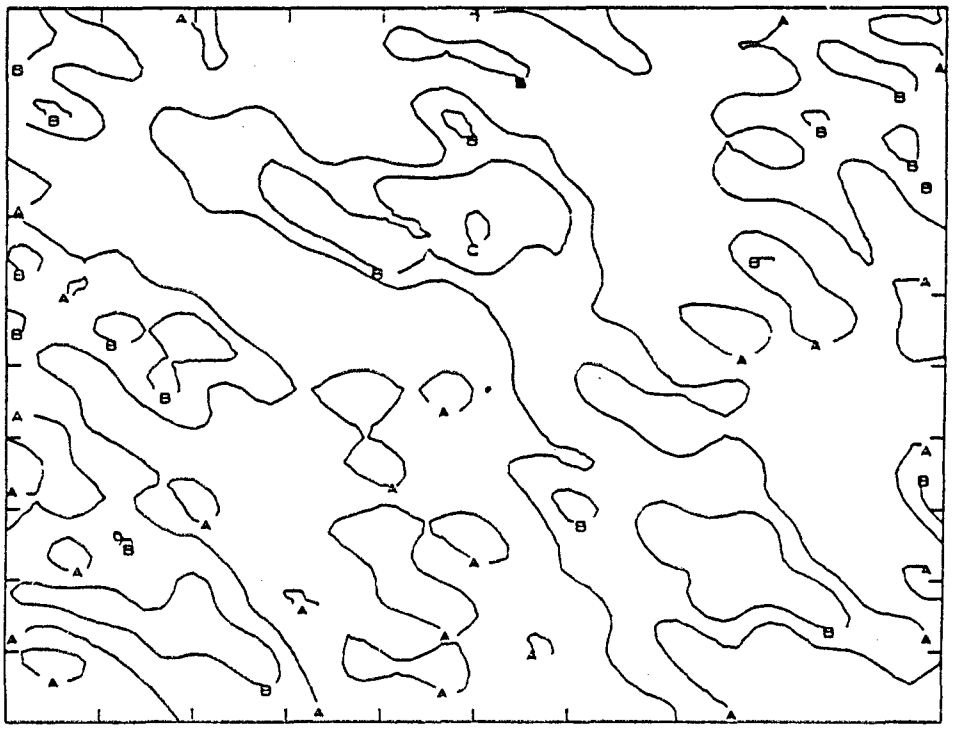

(b) V=18 knots, β_W = 45 deg

Figure 10 — Contour plots of ambient wave elevations

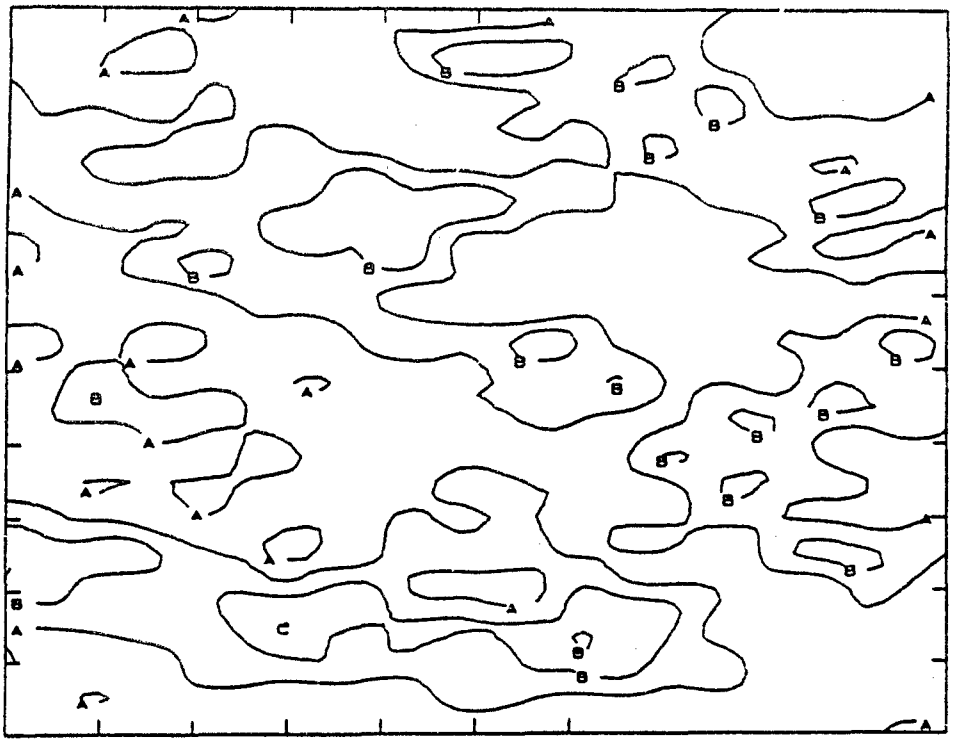

(c) V=18 knots, β_W = 90 deg

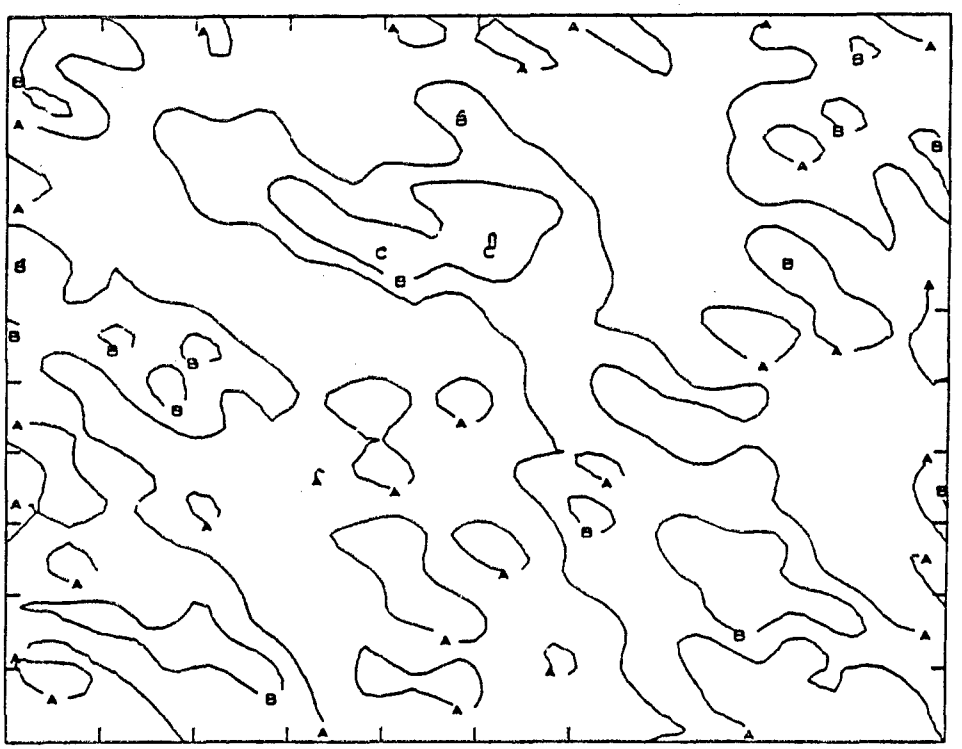

(d) V=12 knots, β_W = 45 deg

Fig. 10 (Continued) — Contour plots of ambient wave elevations

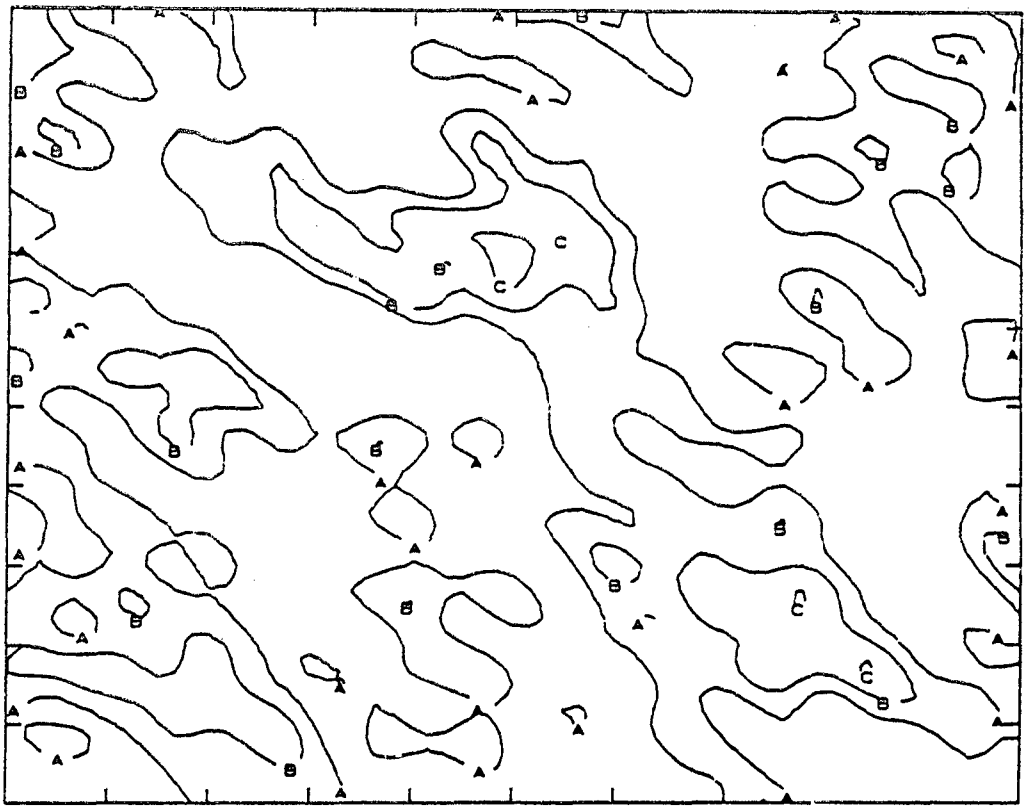

(e) V=42 knots, β_W = 45 deg

Fig. 10 (Continued) — Contour plots of ambient wave elevations

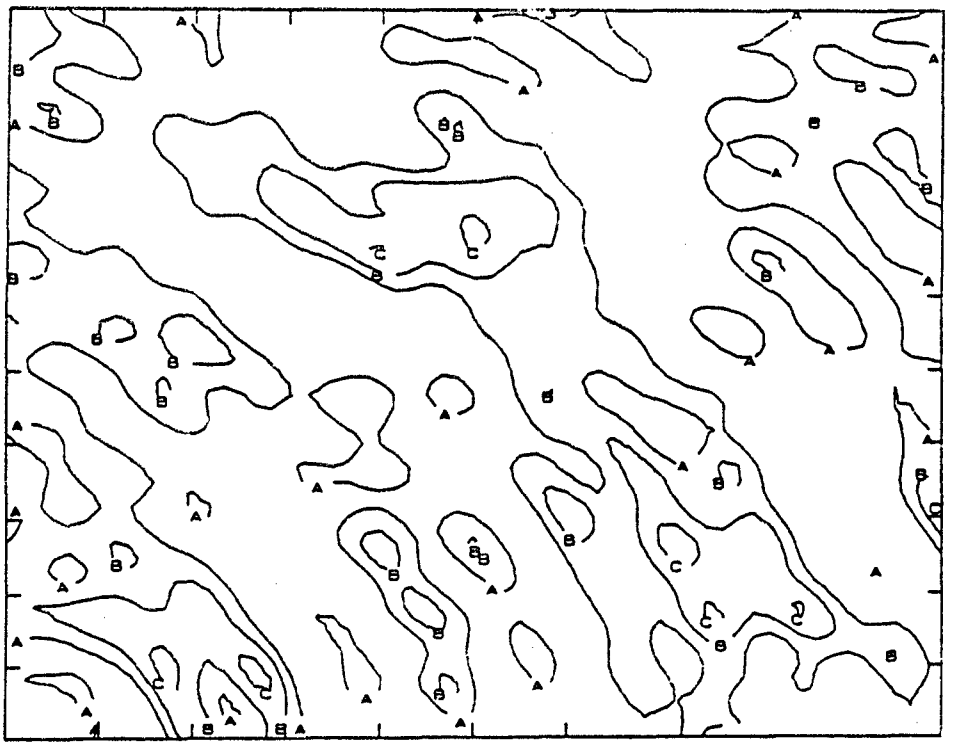

(a) DE1006, V=18 knots, β_W = 45 deg

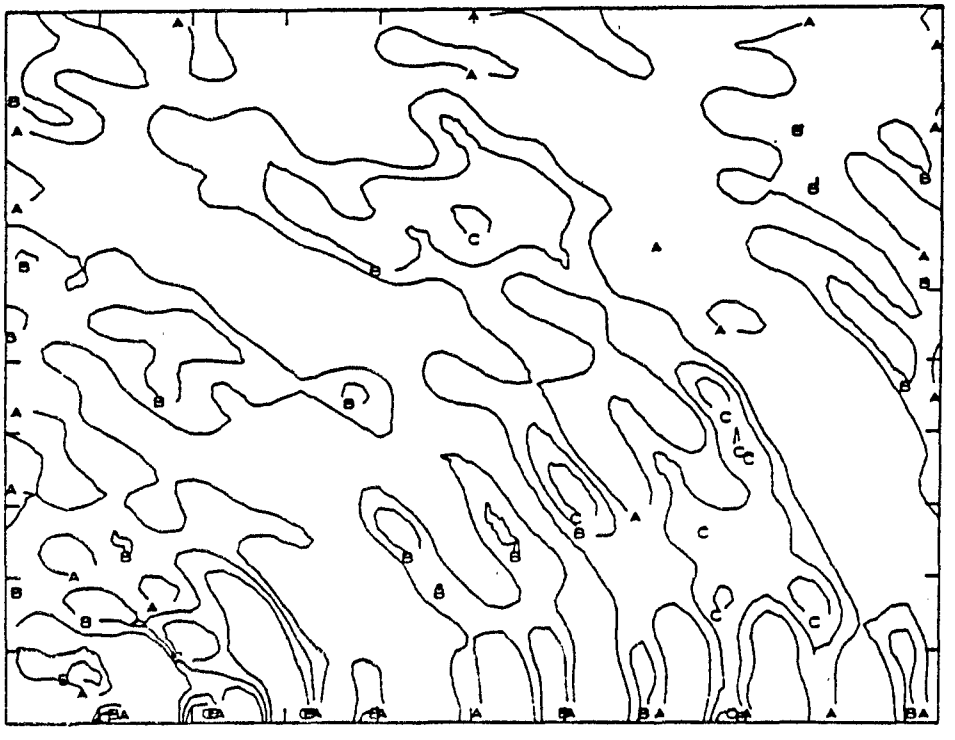

(b) CVA59, V=18 knots, β_W = 45 deg

Figure 11 — Contour plots of superposed ship and ambient wave elevations

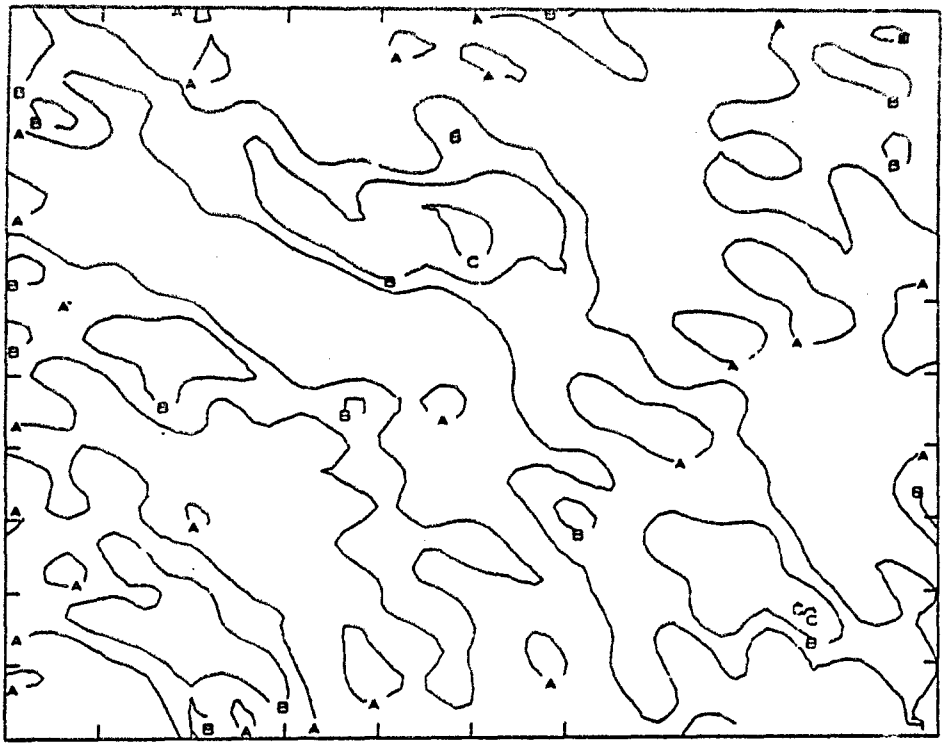

(c) TAGOSTW, V=18 knots, β_W = 45 deg

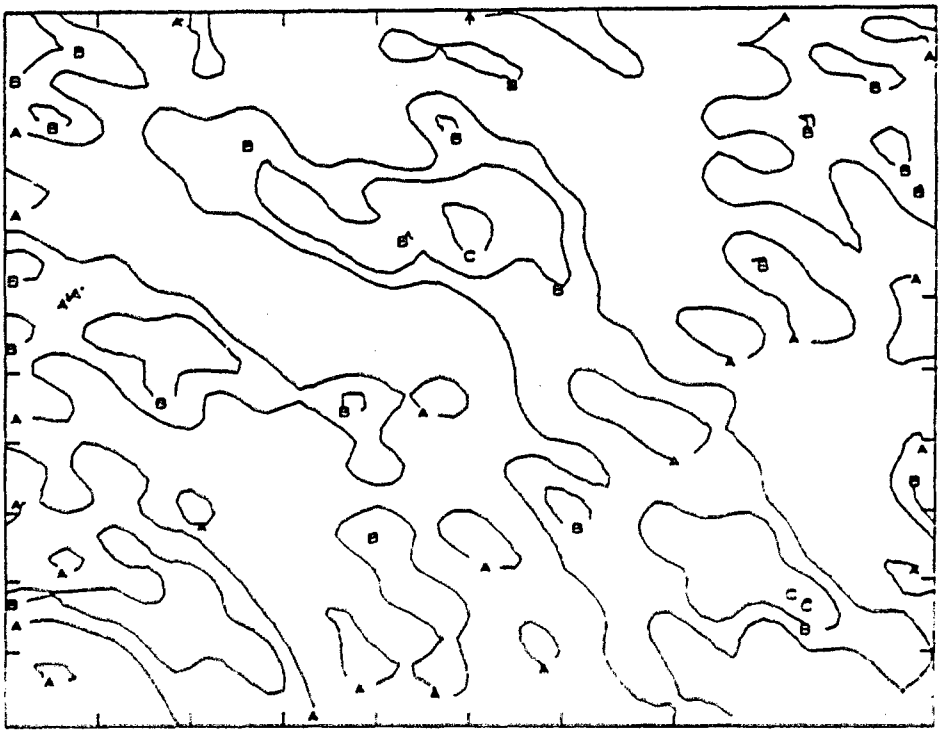

(d) TAGOSMH, V=18 knots, β_W = 45 deg

Fig. 11 (Continued) — Contour plots of superposed ship and ambient wave elevations

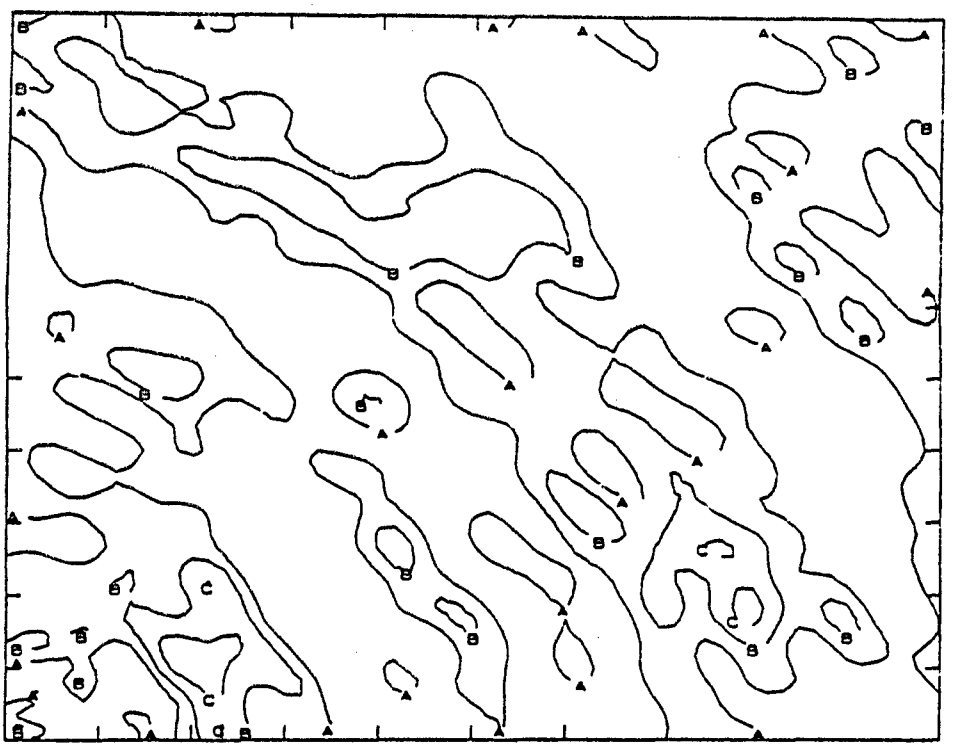

(e) DE1006, V=12 knots, β_W = 45 deg

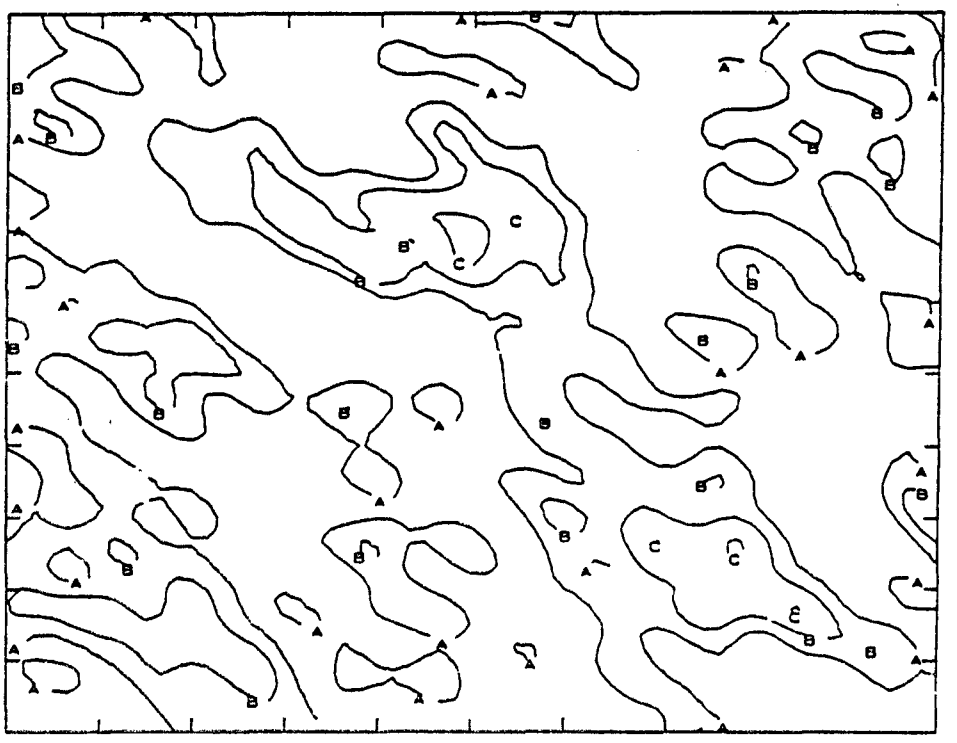

(f) DE1006, V=42 knots, β_W = 45 deg

Fig. 11 (Continued) — Contour plots of superposed ship and ambient wave elevations

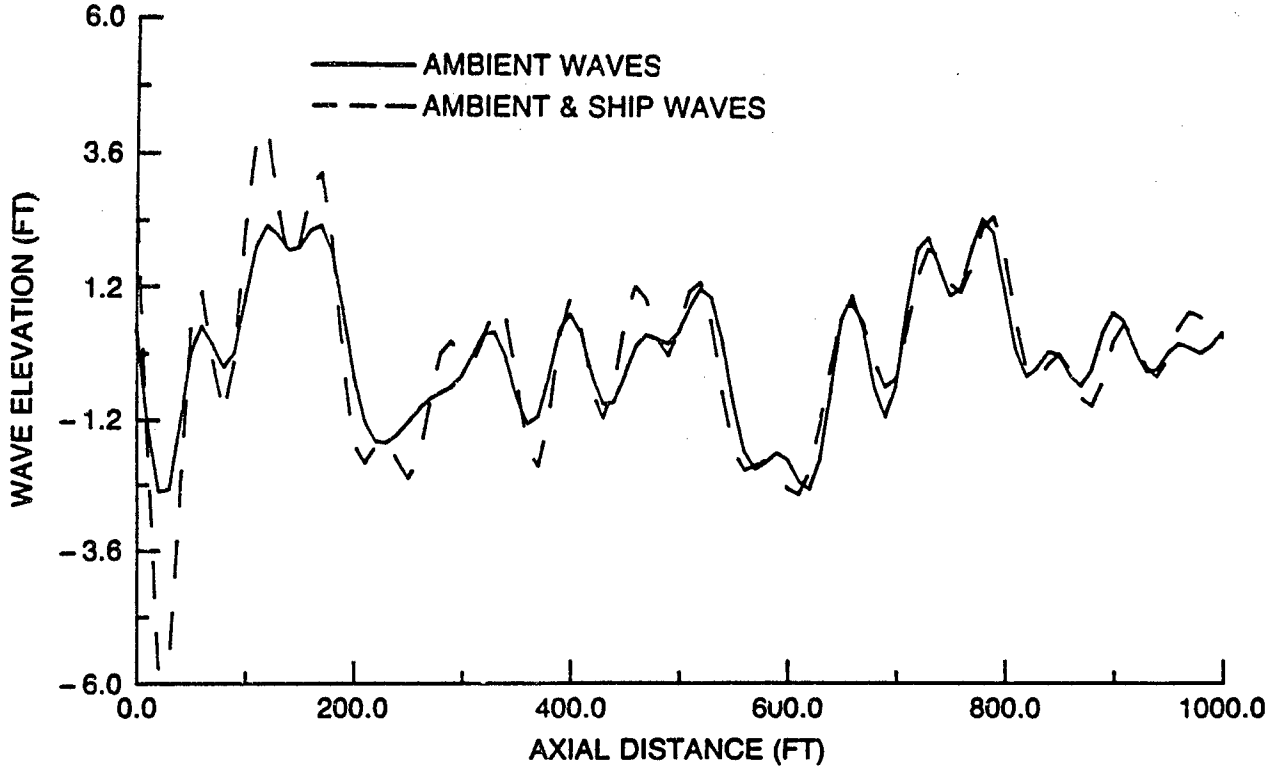

(a) DE1006, α = 0 deg, V=18 knots, β_W = 0 deg

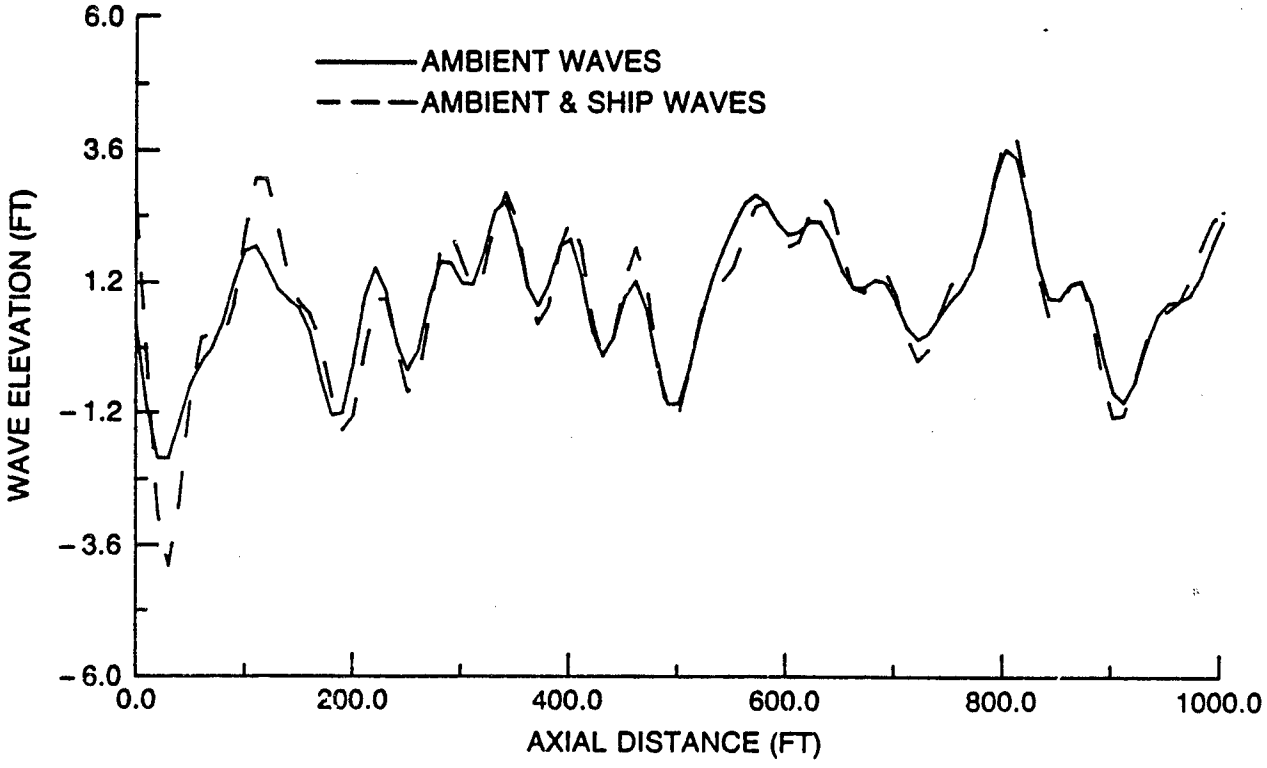

(b) DE1006, α = 45 deg, V=18 knots, β_W = 0 deg

Figure 12 — Two-dimensional plots of ambient, and superposed ship and ambient wave elevations along fixed directions

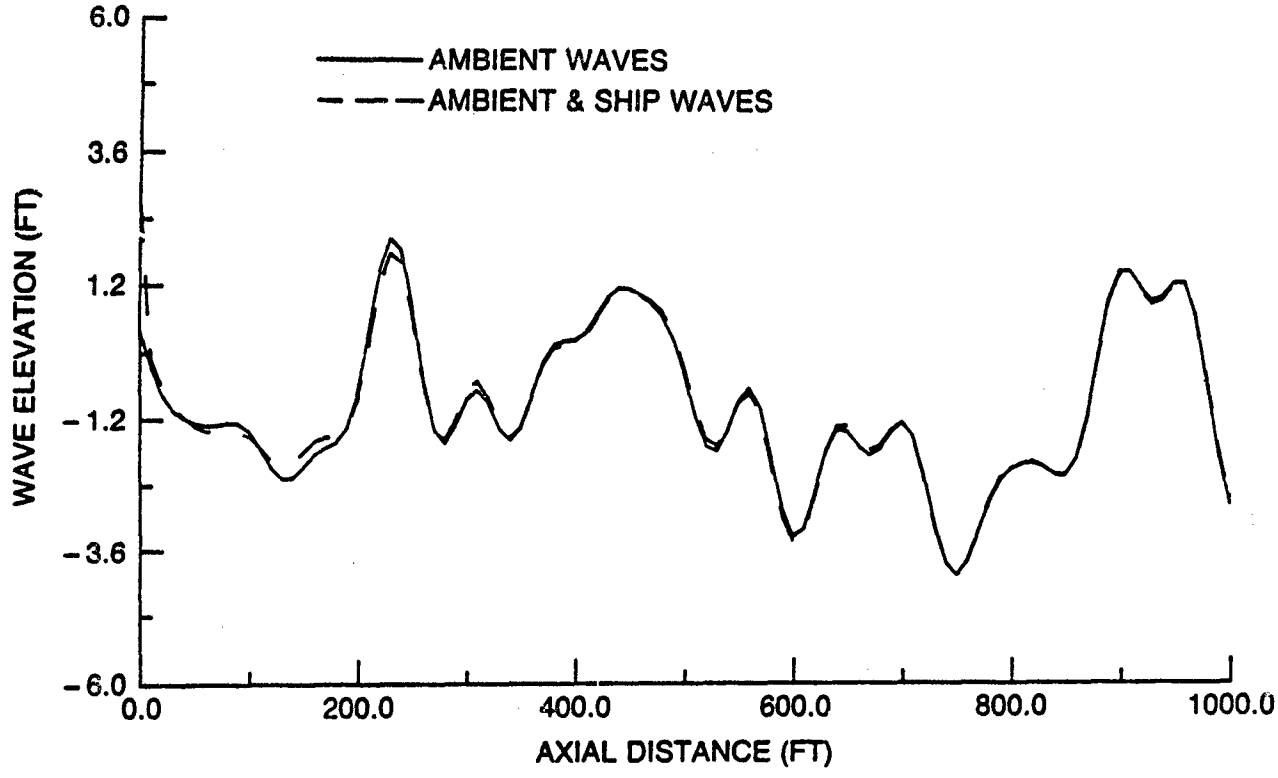

(c) DE1006, α = 90 deg, V=18 knots, β_W = 0 deg

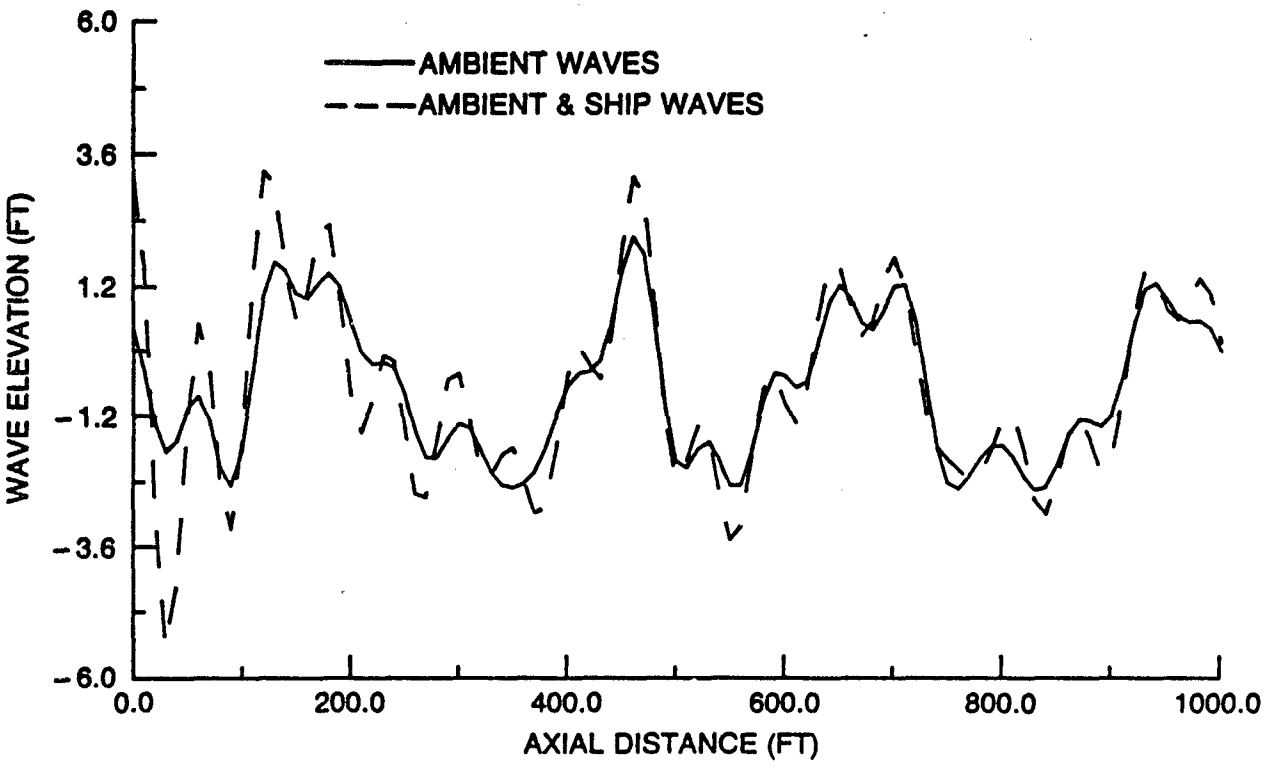

(d) DE1006, α = 0 deg, V=18 knots, β_W = 45 deg

Fig. 12 (Continued) — Two-dimensional plots of ambient, and superposed ship and ambient wave elevations along fixed directions

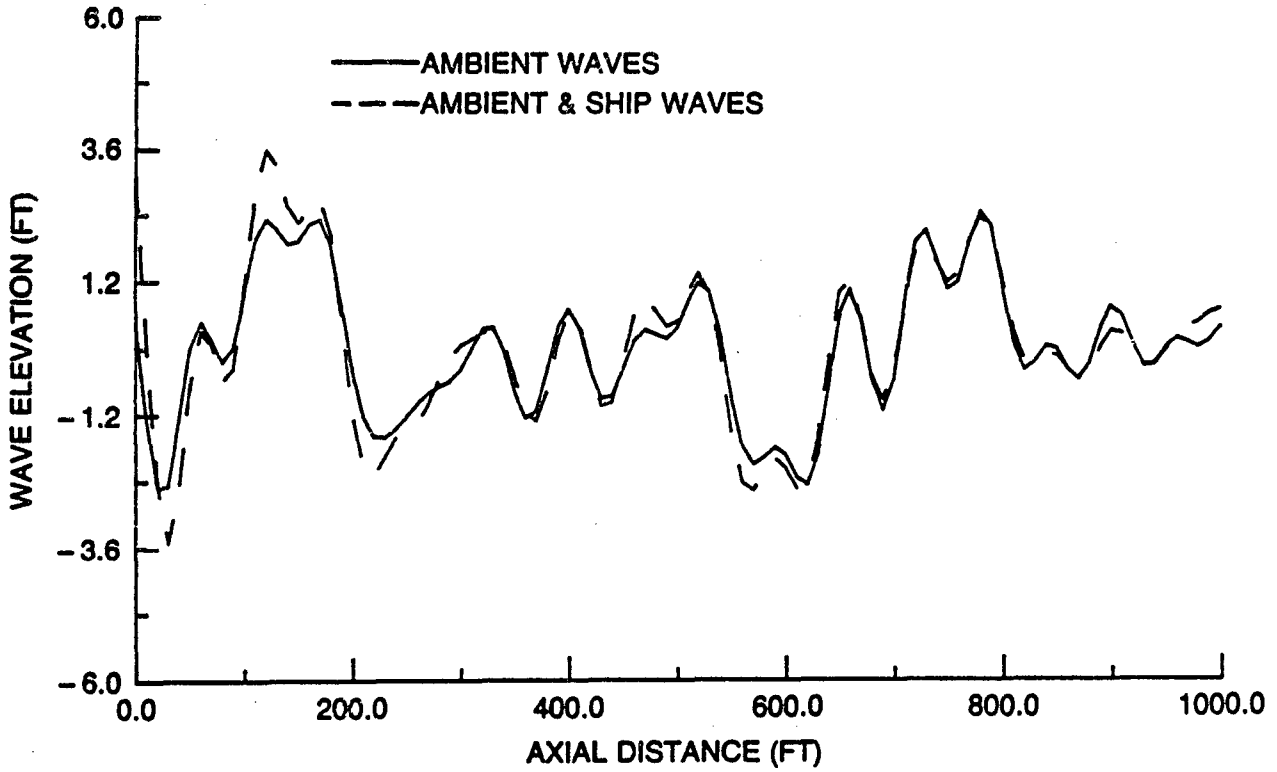

(e) DE1006, α = 45 deg, V=18 knots, β_W = 45 deg

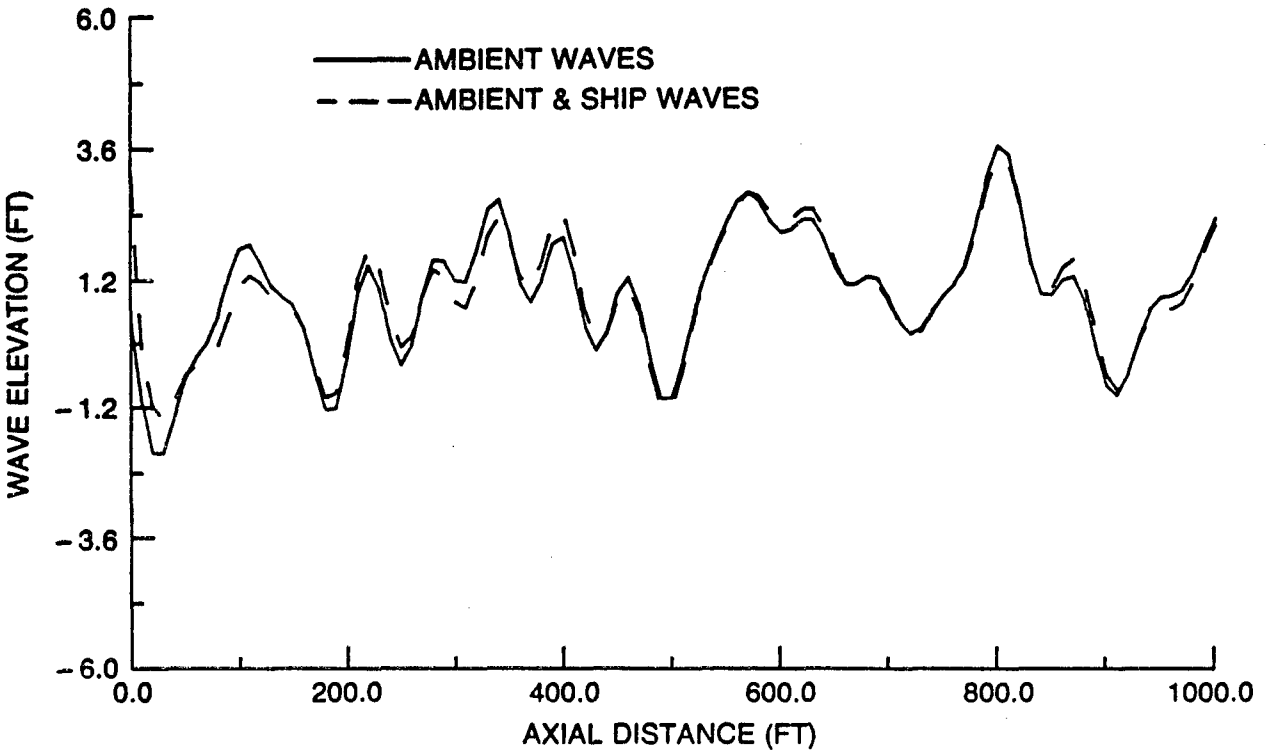

(f) DE1006, α = 90 deg, V=18 knots, β_W = 45 deg

Fig. 12 (Continued) — Two-dimensional plots of ambient, and superposed ship and ambient wave elevations along fixed directions

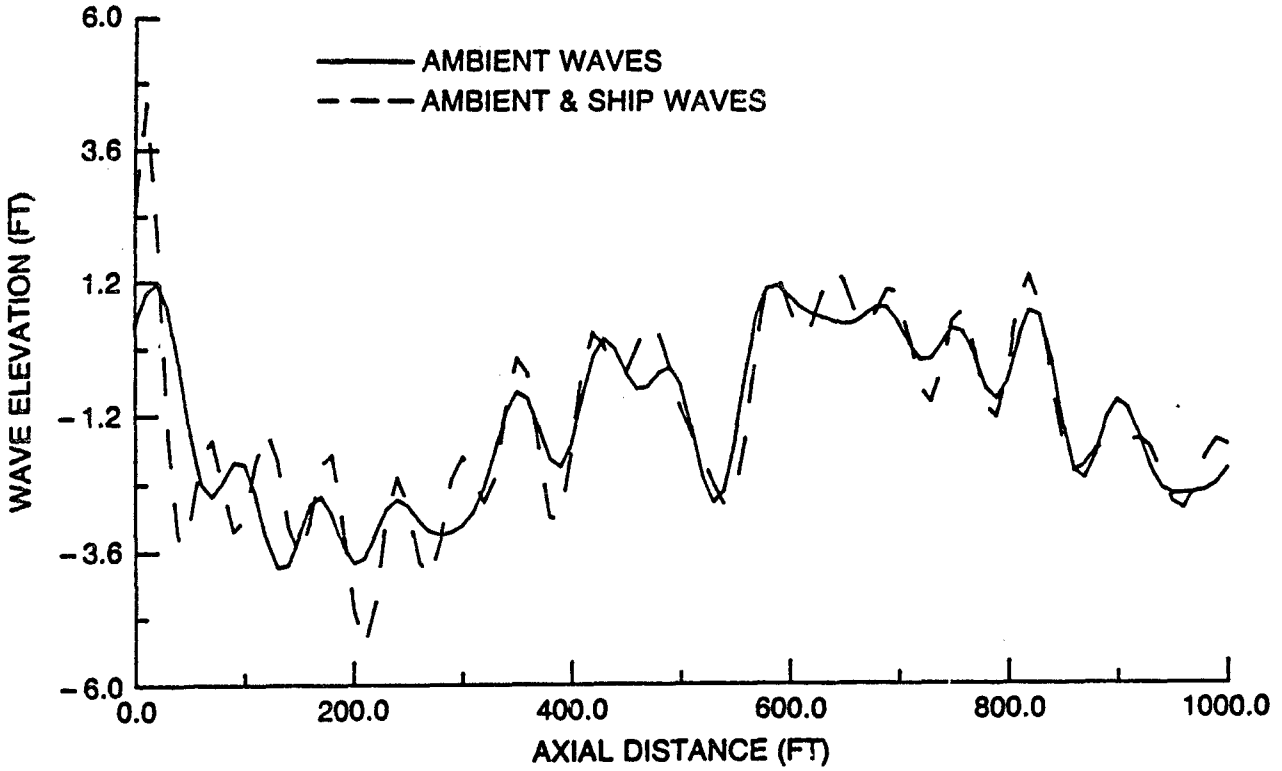

(g) DE1006, α = 0 deg, V=18 knots, β_W = 90 deg

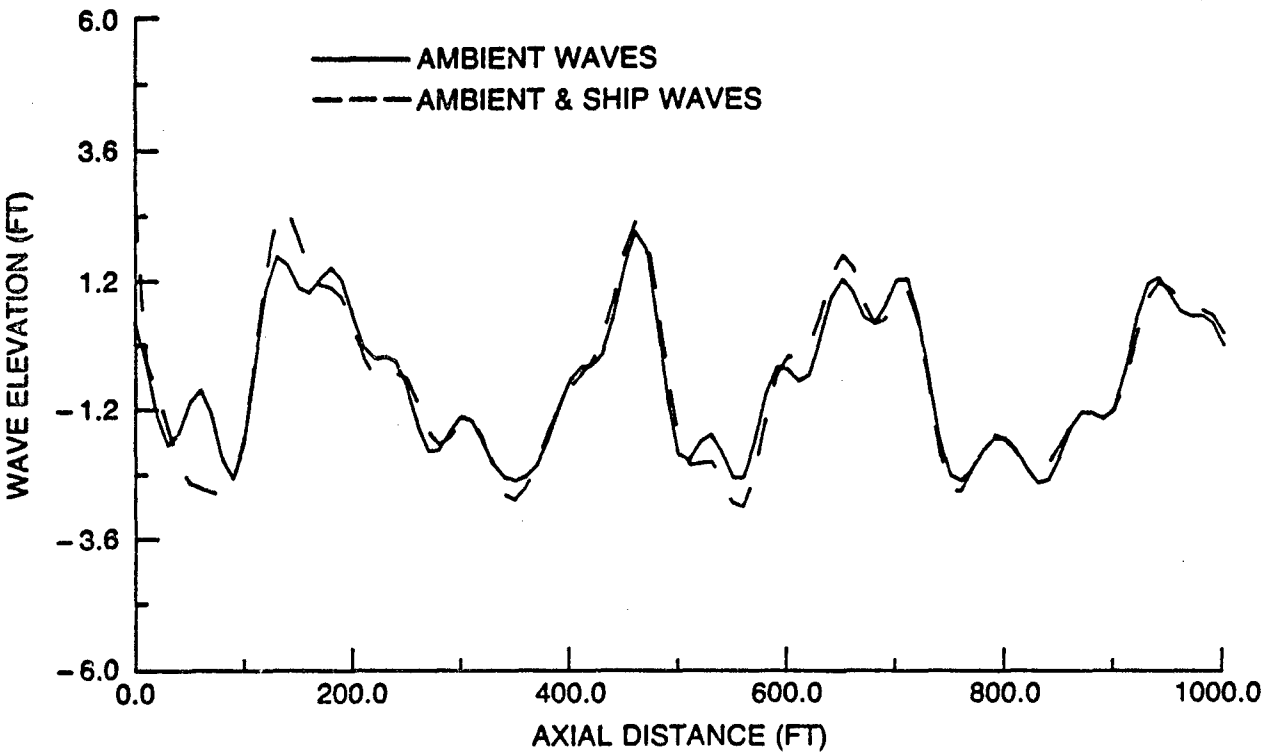

(h) DE1006, α = 45 deg, V=18 knots, β_W = 90 deg

Fig. 12 (Continued) — Two-dimensional plots of ambient, and superposed ship and ambient wave elevations along fixed directions

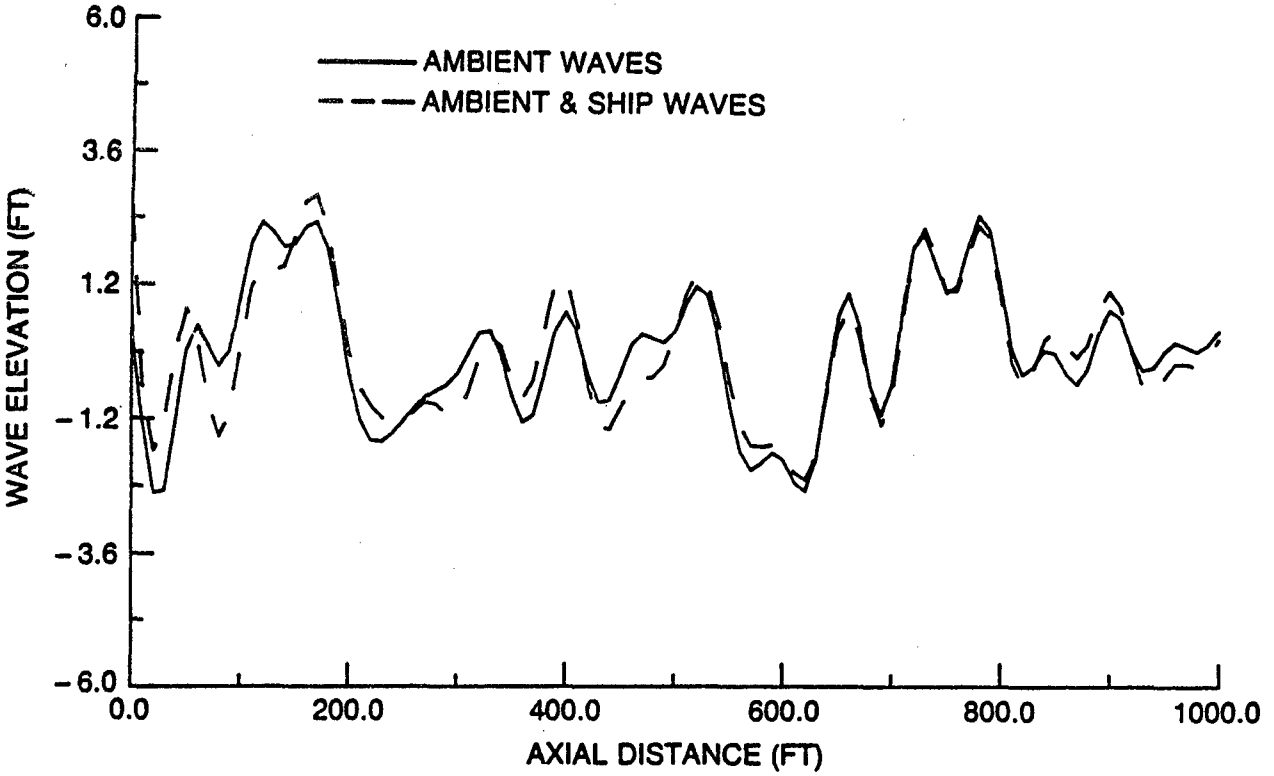

(i) DE1006, α = 90 deg, V=18 knots, β_W = 90 deg

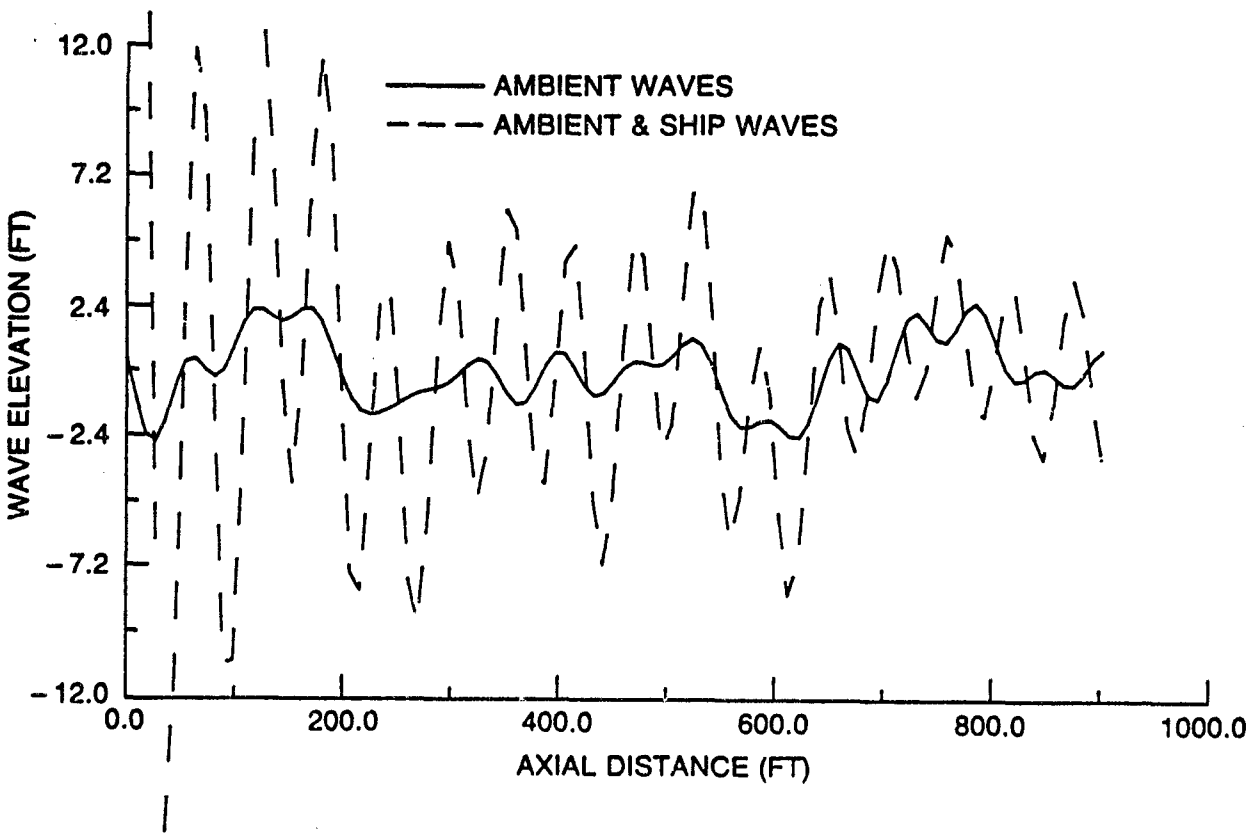

(j) CVA59, α = 0 deg, V=18 knots, β_W = 0 deg

Fig. 12 (Continued) — Two-dimensional plots of ambient, and superposed ship and ambient wave elevations along fixed directions

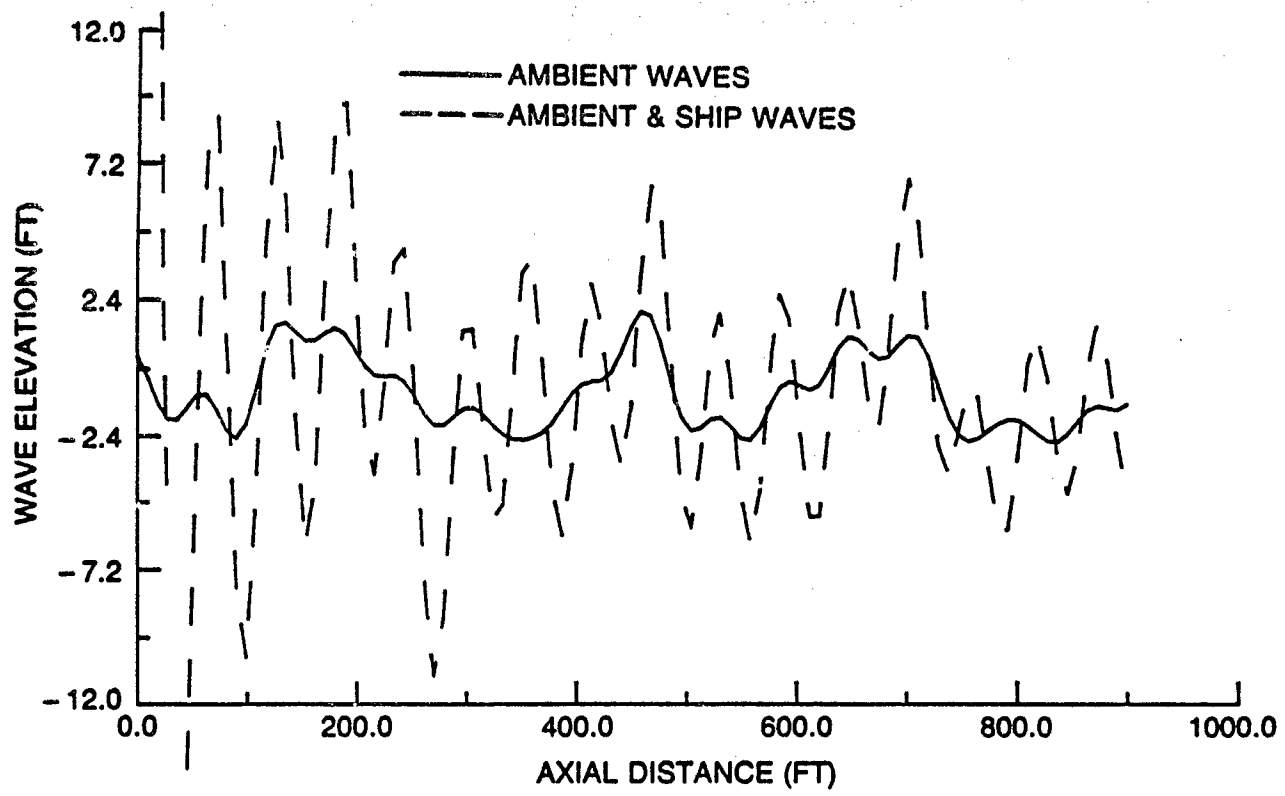

(k) CVA59, α = 0 deg, V=18 knots, β_W = 45 deg

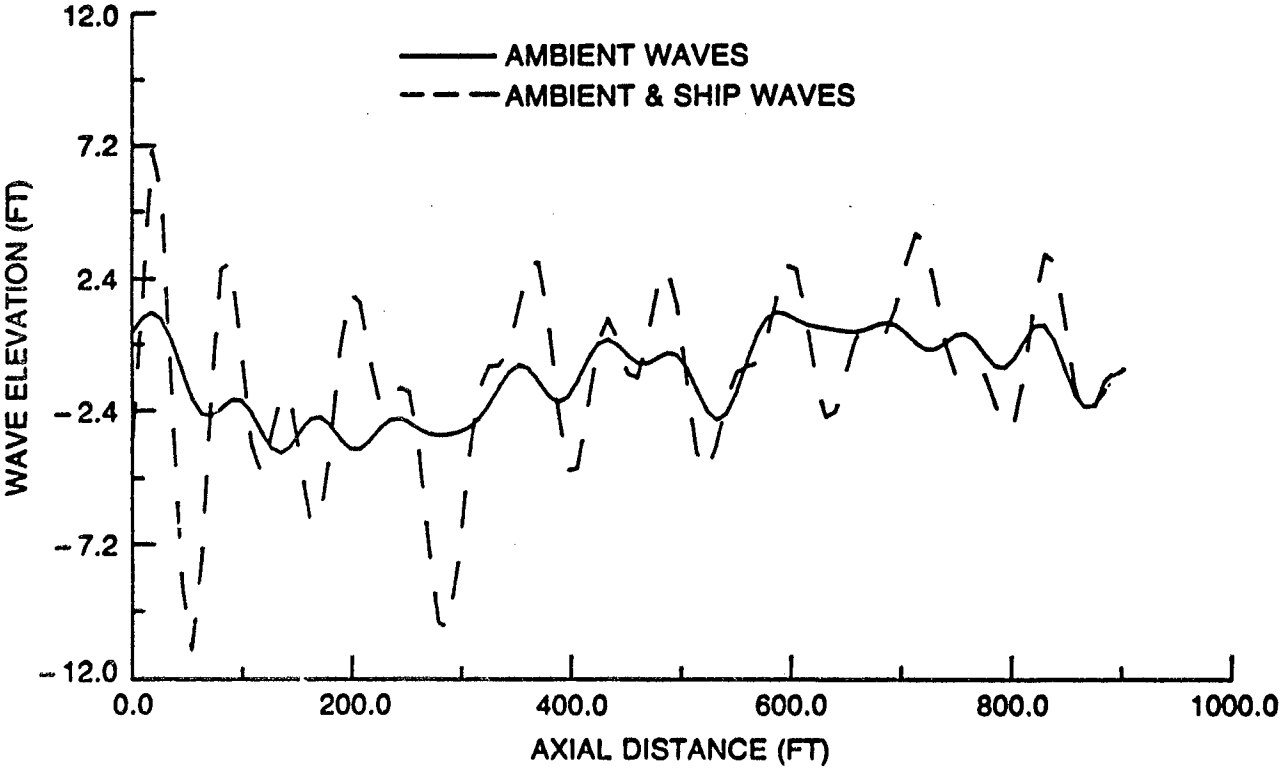

(l) CVA59, α = 0 deg, V=18 knots, β_W = 90 deg

Fig. 12 (Continued) — Two-dimensional plots of ambient, and superposed ship and ambient wave elevations along fixed directions